PART V

BIODEGRADABLE COMPOSITES

CHAPTER 15

Starch-Based Nanocomposites Using Layered Minerals

H. R. FISCHER and J. J. DE VLIEGER

TNO Science and Technology 5600 HE Eindhoven, The Netherlands

15.1 INTRODUCTION

The worldwide production of synthetic plastics is still growing. Out of the total plastics production approximately 40% is used in packaging. This short-term application will cause a global environmental problem because these plastics are not compostable and are difficult to recycle. The limited fossil resources require a renewable alternative that will not eventually contribute to the amount of greenhouse gases. Plastics from renewable resources are in most cases compostable, solving landfill and litter problems. The bioplastics in the market today are used in specific sectors where biodegradability is required such as packaging, agriculture, and hygiene. Bioplastics based on starch exploit the benefits of natural polymerization and the availability of the raw material. They offer a renewable resource for compostable plastics at potentially low and competitive prices.

Starch is nature's primary means of storing energy and is found in granule form in seeds, roots, and tuber cells as well as in stems, leaves, and fruits of plants. The two main components of starch are polymers of glucose: amylose (MW 10^5–10^6),

Biodegradable Polymer Blends and Composites from Renewable Resources. Edited by Long Yu

the major component and an essentially linear molecule; and amylopectin (MW $10^7 - 10^9$), a highly branched molecule. Starch granules are semi-crystalline with crystallinity varying from 15% to 45% depending on the source. The term "native starch" is mostly used for industrially extracted starch. It is an inexpensive (<0.5 euro/kg) and abundant product, available from potato, maize, wheat, and tapioca.

Thermoplastic starch (TPS) or destructurized starch is a homogeneous thermoplastic substance made from native starch by swelling in a solvent (plasticizer, mainly water and/or glycerol) and a consecutive "extrusion" treatment consisting of a combined kneading and heating process. Due to the destructurization treatment, the starch undergoes a thermomechanical transformation from the semicrystalline starch granules into a homogeneous amorphous polymeric material. One of the major problems connected with the use of most natural polymers, especially of carbohydrates, is their high water permeability and associated swelling behaviour in contact with water. All this contributes to a considerable loss of mechanical properties, which prohibits straightforward use in most applications. So far, special processing or after-treatment procedures are necessary to sustain an acceptable product quality. Presently applied methods for decreasing the hydrophilicity and increasing and stabilizing mechanical properties include:

- Application of hydrophobic coating(s) on the surface of bioplastic products
- Blending with different, hydrophobic, biodegradable synthetic polymers (polyesters)
- Reactive extrusion of natural polymers (graft- and co-polymerization, esterification during extrusion process), which diminishes the opportunities for hydrolysis.

The resulting products are, however, rather expensive compared with common alternative plastics. New concepts are required to solve the intrinsic problem of the hydrophilicity and mechanical instability of starch-based bioplastics without too much added cost. Application of the nanocomposite concept has proved to be a promising option in this respect. Moreover, the combination of two materials from a renewable/totally natural source into a new engineering material with enhanced properties, as in the case of combination of starch and natural clay as nanocomposite materials, offers a new concept in dealing with environmental problems caused by extensive use of disposable plastic products.

This chapter focuses on starch-based nanocomposites using layered minerals. An extensive review of developments in nanocomposites with many other biodegradable polymers as well has recently been published (Yang et al., 2007).

15.2 STARCH–MONTMORILLONITE NANOCOMPOSITES

For the preparation of nanocomposite materials consisting of a polymer and clay, it is necessary to use special compatibilizing agents (modifiers) between the two

basic materials. However, since starch is plasticized mostly by compounds capable of hydrogen bonding and organized by the formation of (multiple) hydrogen bonds, such as water, glycerol, and amines, during processing at elevated temperatures, those plasticizers may also be used for distribution of the clay platelets. Amorphous starch recrystallizes upon storage, and the crystal form developed as well as the crystallinity depend on the water content. In order to achieve the final clay–starch nanocomposite material, "clay modification" and "extrusion" processing steps can be distinguished; these are described below.

The starch and the modified or preswelled clay can be mixed at temperatures above the softening point of the polymer by polymer melt processing (extrusion) to obtain exfoliated nanocomposite materials. Fully destructurization is needed for successfully polymer melt processing of starch.

The process of clay exfoliation requires essentially a modification of the surface such that the interlayer width exceeds some threshold value that depends on the difference of absorption energy in order to be thermodynamically favorable (Kudryavtsev et al., 2004). For exfoliation in the presence of starch, spontaneous mixing of (modified) clay and starch is required with enthalpic interactions between TPS and modifier units being favorable. Hydrophilic compounds such as the plasticizers mentioned earlier also interact strongly with the remaining ions found in the galleries of natural clay or with hydrophilic clay modifiers that might be used to meet these conditions and allow exfoliation to occur.

The following reports of studies present various attempts to obtain exfoliated structures in order to find a relation between improved properties and the nanocomposite structures.

True starch nanocomposites were first described in a study in which potato starch and modified clay were mixed above the softening point of starch by polymer melt processing (extrusion) (Fischer et al., 2001). The screw speeds were shown to be of great importance for the clay dispersion. The higher the screw speed, the better the dispersion of the clay particles within the starch matrix. TEM analysis showed an excellent and homogeneous distribution of the individual clay sheets (see Fig. 15-1). Sample preparations are not extensively described but no agglomerations of clay were found in X-ray diffraction (XRD) analysis. The resulting retrogradated materials displayed remarkable stability against cold water; no swelling occurred, and blown film bags filled with water retained their mechanical integrity and did not leak over a period of about 3 weeks. The clay in the starch–clay nanocomposite certainly affected the water stability properties (see Fig. 15-2).

TPS samples consisting of starch/water/glycerol in the proportions 5/2/3 were premixed at 110°C for 25 min in a Haake mixer, then cooled, cut and dried, and mixed with predried clays (three organically modified montmorillonite [MMT] with different ammonium cations, and one unmodified Na^+MMT [Cloisite Na^+] were used); the content of clay ranged from 2.5 to 10 wt% at 110°C (Park et al., 2002, 2003). The blends after preparation were placed in a sealed bag to prevent any moisture absorption. Only some partial intercalation was detected by XRD analysis; the samples containing the nonmodified clay showed hardly any intercalation with the starch. The modification of the clays does not match well thermodynamically

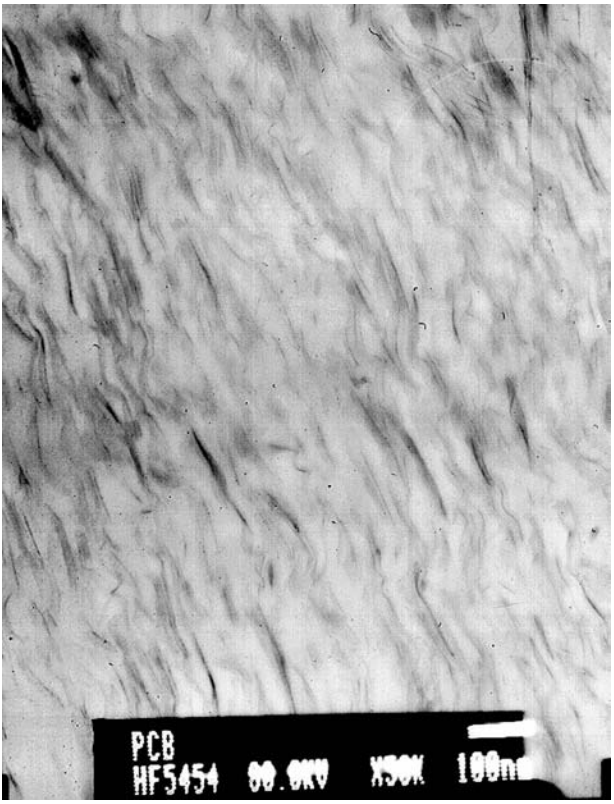

Fig. 15-1 TEM image of a TPS/5% montmorillonite nanocomposite plasticized with 30% glycerol/18% water, showing excellent exfoliation of the clay sheets and a homogeneous distribution and alignment after extrusion direction. (After Fischer et al., 2001.)

with the TPS matrix, and consequently the dispersion is poor. Although the tensile strength for all samples was almost the same, a slight increase was reported again for the samples containing the nonmodified clay (3.3 MPa instead of 2.6 MPa), together with slightly enhanced water vapor barrier properties.

A matrix of four different types of starches and three different clay samples have been studied for their ability to form nanocomposite compositions (Chiou et al., 2005). The samples were prepared by first adding the nanoclays (the hydrophilic Cloisite Na^+ clay as well as the more hydrophobic Cloisite 30B, 10A, and 15A clays) in concentrations of 2.5, 5.0, 7.5, and 10 wt% relative to starch. This starch–nanoclay powder was mixed manually in a plastic bag and the moisture content, up to 51 wt%, was then adjusted with deionized water. One particular sample also contained 15 wt% glycerol and only 36 wt% water. However, under such conditions it is not likely that exfoliation takes place. After mixing at room temperature, samples were analyzed in dynamic tests and creep tests using parallel plates and by XRD analysis.

Fig. 15-2 A bag manufactured from a blown film of a TPS/5% montmorillonite nanocomposite plasticized with 30% glycerol/18% water. The bag was filled with water and stored for 20 days, showing excellent stability against cold water. (After Fischer et al., 2001.)

In short, at higher clay concentrations the Na-Cloisite samples had larger, frequency-independent elastic moduli and lower creep compliances than the other samples, indicating that these samples formed more gel-like materials. During analysis at higher temperatures (where gelatinization occurred), amylose that leached from the granules interacted more with the clay interlayers than was the case for the other clay samples. Potato starch samples showed a higher swelling capacity than other starches. This produced softer granules and led to lower elastic moduli in the clay–starch mixtures.

It is clear that major steps in improvement of mechanical properties can be achieved only if true nanocomposites are formed in the sample preparation steps.

Similar results were obtained when chitosan was used as a compatibilizing agent in order to disperse clay particles in a starch matrix (Kampeerapappun et al., 2007). Samples were prepared as follows: 100 parts of a mixture of starch with 0–15 wt% of chitosan and 1–15 wt% clay were mixed with 20 parts of glycerol. Distilled water was also added, followed by acidification with acetic acid to 1% (v/v) in order to dissolve the chitosan. The mixture was then heated to the gelatinization temperature of 70–80°C for 1 hour. The starch solution was cast onto an acrylic sheet mold with a wet thickness of 3 mm and dried overnight. For most analyses samples were conditioned at 50% RH at 23°C. XRD of samples of chitosan-treated MMT shows an increase in interlayer space from 14.78 to 15.80 Å. The starch composite films display a peak at 5.015° which corresponds to an interlayer space of 17.62 Å. This shift was due to the intercalation of glycerol in the clay. However, a completely

exfoliated structure usually results in complete loss of registry between the clay layers. Consequently, SEM images show (large) aggregates of clay particles.

The tensile strength of the samples is remarkably high even for the free starch film; addition of MMT has hardly any effect and films containing chitosan show some increase in strength, from 21 MPa in starch/clay films to 25 MPa in starch/clay/chitosan films. Also the Young's modulus was quite high for these type of samples (1000 MPa), but the elongation at break was very low (only 5%). Perhaps this can be attributed to a quite low content of plasticizer in the samples. The water vapor transmission rates decreased from 2000 to 1082 g m^{-2} day^{-1} depending on the chitosan content. It was concluded that residual acetyl groups played an important role in hindering transport of water vapor due to reduced surface wettability. Similarly, the moisture absorption rates decreased significantly from 125% to 61% with respect to chitosan contents of 0 and 20 wt%, respectively.

The incorporation of nanoclay sheets into biopolymers can in general have a large positive effect on the water sensitivity and related stability problems of bioplastic products (Fischer et al., 2001). The nature of this positive effect lies in the fact that clay particles act as barrier elements since the highly crystalline silicate sheets are essentially impermeable even for small gas molecules such as oxygen or water, which has a large effect both on the permeation of incoming molecules (water or gases) and for molecules that tend to migrate out of the biopolymer, such as the water used as plasticizer in TPS. In other words; a nanocomposite material with well-dispersed nanoscaled barrier elements should show not only increased mechanical properties but also increased long-term stability of these properties and a related reduction of aging effects.

Mixing of wheat starch plasticized with 36 wt% glycerol and montmorillonites modified with aminododecanoic acid, stearyl dihydroxyethyl ammonium chloride, and distearyldimethyl ammonium chloride did not lead to true nanocomposite materials (Bagdi et al., 2006). The modified clays were swollen in glycerol for 1 day, homogenized with the starch powder, and processed in a mixer at 150°C for 10 min. Plates were compression-molded from the melt at 150°C in 5 min and stored under dry conditions. The swelling of the clay in glycerol resulted in some competitive dissolution adsorption of the plasticizer but not in exfoliation. The clay modification used in this study is certainly not optimal for generating nanocomposites and the mixing step might require more shear force for the intercalation and exfoliation process to reach favorable thermodynamic conditions. It was also found that the T_g of the composites is around 40°C, indicating that hardly any retrogradation can occur. The majority of the thermoplastic starch was found to be amorphous, but some crystallinity different from that of neat starch was found.

Thermodynamic conditions for preparing nanocomposites starting with organoclay are better when thermoplastic acetylated starch (TPAS) is used instead of neat TPS (Qiao et al., 2005). Compositions of acetylated starch/glycerol/clay with weight ratios 100/50/5 are described. The three components were mixed by hand and sealed for 12 h to effect sufficient swelling. The mixture was processed at 150°C for 10 min in a roller mixer. The composites obtained were hot pressed at 160°C to achieve samples of 1 mm thickness, the samples were stored in tightly

sealed polyethylene bags to prevent moisture absorption. The intercalation of the TPS into the clay layers has been demonstrated by XRD; the tensile strength increased as expected from 5.5 to 10.3 MPa compared with TPAS and TPAS/OMMT; and the elongation at break decreased, also as expected. The storage modulus decreased rapidly above the T_g of 50°C due to the action of the layered silicates; however, the T_g was increased by the incorporation of clay.

Other approaches to obtain starch clay nanocomposites using montmorillonite with different modifiers and differently plasticized starches have been described in several studies from one academic group (Huang et al., 2004, 2005a,b, 2006; Huang and Yu, 2006). Here, conditions for deriving true nanocomposites were still not favorable, because a single-screw extruder was used for mixing and shear forces were perhaps not high enough.

Glycerol-plasticized thermoplastic starch was used to manufacture montmorillonite-reinforced starch composites (Huang et al., 2004). The samples were made by premixing glycerol and starch with a mixer and then stored in tightly sealed bags for 36 h, and the swelled mixtures were subsequently fed into a single-screw extruder and cut into small particles. These particles were again mixed with clay in the single-screw extruder. The blends were stored in sealed polyethylene bags. The clay was found to be uniformly dispersed in the starch on a submicrometer scale. The introduction of clay decreased the water absorption of the composites. The tensile strength of samples with a clay content of 30% stored at 39% RH for 2 weeks reached 27 MPa. Most importantly, the clay restrained crystallization of the starch for a long time (>90 days).

Similar behavior was found in formamide/ethanolamine-plasticized starch together with ethanolamine-activated clay (Huang et al., 2005a,b). Formamide was dissolved in the ethanolamine and the solution was premixed with the starch to form compounds with total 30% plasticizer calculated on weight starch. The preparation of nanocomposites was the same as described above. SEM and TEM showed that montmorillonite layers were expanded and uniformly dispersed in the nanometer range, and intercalated nanocomposites were formed. When the content of clay is in the range 2.5–10% the mechanical properties are clearly improved. Samples were stored at 25% RH before use for 2 weeks. The tensile strength increased from 6.5 to 9.7 MPa, the yield stress from 5.1 to 8.5 MPa, and the modulus from 68 to 184 MPa, while the elongation at break decreased from 88% to 74%.

The postcrystallization of starch was affected only by the incorporation of clays. This is not surprising since postcrystallization can only occur with sufficient moisture present. In general, starch crystallization cannot be avoided but is detrimental in maintaining good mechanical properties because the material becomes more brittle in time.

The nanoplastics prepared in the latter study (Huang et al., 2005a) showed restrained crystallization behavior when samples were stored at RH 50% for 30, 60, and 90 days. It was shown that the formamide and ethanolamine plasticizers did not impede the crystallization behavior of thermoplastic starch and it was concluded that the clay sheets must influence this noncrystallization behavior. Samples with clay were further found also to be more thermal stable. The water absorption

at RH 75% and 100% was found to be lower than in the nanocomposites with the plasticized starch.

The conditions for nanocomposite formation were much better when starch was plasticized with urea and formamide and the clay was activated with citric acid. The *d*001 peak in the XRD pattern completely disappeared, indicating that the crystal lattice structure of the clay was totally dispersed and the slice layers exfoliated in the thermoplastic starch (Huang et al. 2006). The tensile stress with 10 wt% clay was highest, with a value of 24.9 MPa. The nanocomposite with 5 wt% clay had the maximal tensile strain 134%. The effect of water content on mechanical properties was also measured. Increasing of water content from 5% to 35% caused first an increase the tensile stress and then a decrease; the maximal tensile stress of nanocomposites reached 23 MPa at a water content of 17%. Intercalation of monmorrilonite (MMT) with sorbitol in a single screw extruder as a first step followed by mixing with starch as matrix, sorbitol and formamide leads to composite materials with an increase in tensile modulus by the factor of 4 at a load of 10% MMT together with an increase in strength (factor 3) and only a slight decrease in elongation at break (138 to 93%) (Ma et al., 2007).

Another study used two different clays, sodium montmorillonite (Na-MMT) and sodium fluorohectorite (Na-FHT) (Dean et al., 2007; Yu et al., 2007). It was shown that there was an optimum level of both plasticizer and nanoclay to produce a gelatinized starch film with the highest levels of exfoliation and consequent superior properties.

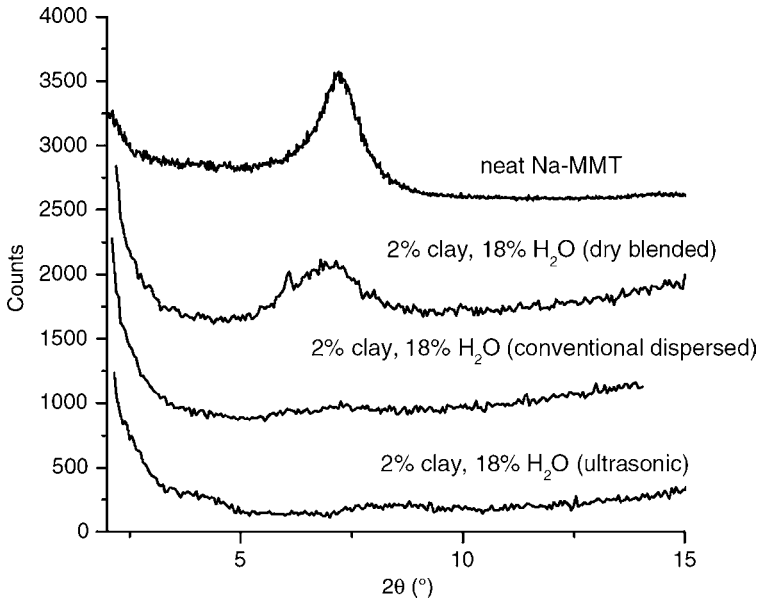

Fig. 15-3 XRD traces for a series of medium water content (18 wt%) Na-MMT/gelatinized starch nanocomposites with 2 wt% clay. (After Dean et al., 2007.)

Nanoclays were mixed with starch by dry blending (DB), or conventional dispersing in water using conventional mixers (CD), or dispersing in water using ultrasonics (U). The water (in the case of DB formulation) or water/clay dispersions were then added dropwise to the starch in a high-speed mixer prior to extrusion. A twin-screw extruder was used to process the starch nanocomposites using a profile producing a melt temperature of 110°C. The starch nanocomposite was extruded directly into sheet form via a 0.5 mm die. This study showed that there was an optimum level of both plasticizer and nanoclay for each type of clay under the conditions used, where exfoliated nancomposites are formed after extrusion only when hydrophilic clays are used and enough water is present.

X-ray analysis showed an increase in intergallery separation ranging from 15.5 Å to 62 Å, depending on water content during sonification prior to extrusion; the latter value was observed for a clay/water ratio of 1 : 10. Similar results were obtained for Na-MMT and Na-FHT. The extruded samples showed complete exfoliation only when enough water (18 wt%) was used in the case of the hydrophilic Na-MMT (with 2 wt% Na-MMT complete exfoliation was achieved, for 3.2 wt% clay some agglomerates are present) but not when using the more hydrophobic Na-FHT (Fig. 15-3).

The most significant improvement in moduli was observed for higher levels of clay (2.6–3.2 wt%), from 2500 MPa for native starch up to 5000 MPa for the nanocomposite. Similar improvements were observed for yield strength from 30 MPa up to 55 MPa (Fig. 15-4). The elongation at break decreases, not unexpectedly, comparing the nanocomposites with neat starch samples. This was explained as follows: Once melt extruded, the thermoplastic starch begins to undergo retrogradation, causing embrittlement and thus reducing the break elongation. On the other hand, clay

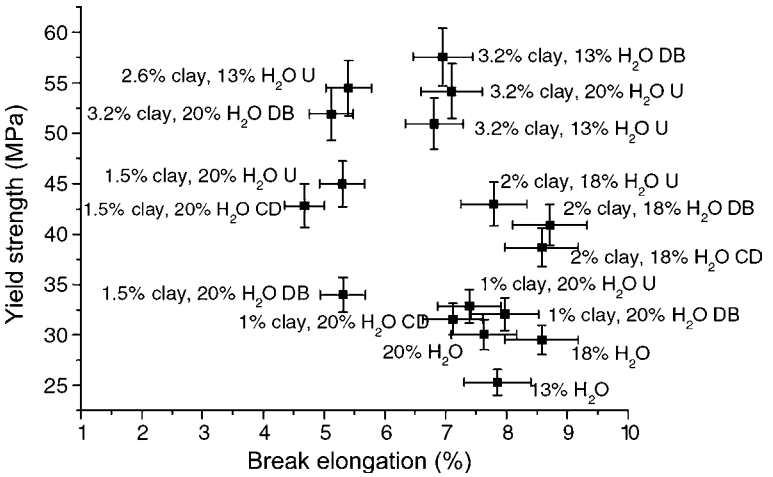

Fig. 15-4 Yield strength versus break elongation for Na-MMT/gelatinized starch nanocomposites for various clay loading, water loadings, and dispersion methods (DB, clay and starch dry blended; CD, clay dispersed using conventional mixing; U, clay dispersed using ultrasonics). (After Dean et al., 2007.)

retains moisture in the sample, leading to a more plasticized material with a greater elongation at break. Consequently a peak in the elongation at break at 2 wt% clay content was observed. For the Na-FHT samples, the yield elongation decreased with increasing clay content, indicating that the Na-FHT was not capable of disrupting recrystallization or binding water tightly into the matrix. Similar trends were observed for the yield strength. Here, the 2.6–3.2 wt% nanocomposites containing 13 wt% water showed the best ratio of strength to elongation.

The order of addition of components in preparing nanocomposites can be of great importance to the final properties of the product and Pandey and Singh 2005 investigated the effect of addition of components, in particular the plasticizer in relation to starch and clay. Glycerol and starch both enter the clay galleries, but it was found that glycerol is favored due to its smaller molecular size. The filler dispersion became highly heterogeneous and the product became more brittle if starch was plasticized before filling with clay. Better mechanical properties were obtained if the plasticizer was added after mixing the clay in the starch matrix. Starch/clay/glycerol was mixed in the four following ways:

1. Starch was gelatinized with water followed by plasticization and then clay slurry was added. This mixture was heated for 30 min to boiling (STN1).
2. A clay slurry in water was mixed with starch in water and heated to boiling, followed by addition of glycerol (STN2).
3. Starch, clay slurry, and glycerol were mixed and heated to boiling (STN3).
4. Glycerol was mixed with clay slurry, stirred for 5 hours, mixed with starch, and heated to boiling (STN4).

Solutions were poured into Petri dishes, water was evaporated, and films of 150–200 μm thickness were obtained and equilibrated at defined RH and temperature. XRD analysis showed the highest increase in d spacing for STN2 and the smallest for STN1. In the latter, probably large structures had formed which negatively affected global mobility. The gallery height was not increased after plasticization, suggesting that the plasticizer can be accommodated among the starch chains. The modulus increased slightly from 790 MPa for neat plasticized starch to 820 MPa for the best nanocomposite sample. The maximum strain was highest at 12% for STN2 and lowest at 6% for STN1, with neat starch having 10%.

In conclusion, better dispersion of clay can be achieved by mixing of starch and filler first, followed by plasticization.

15.3 STARCH-BASED NANOCOMPOSITES USING DIFFERENT LAYERED MATERIALS

Preliminary insight on composites of thermoplastic starch and kaolinite was reported by Carvalho et al. (2001) while studying the use of kaolinite as filler reinforcement for thermoplastic starch to improve its mechanical properties. The composites were prepared using regular cornstarch plasticized with 30% glycerin and hydrated

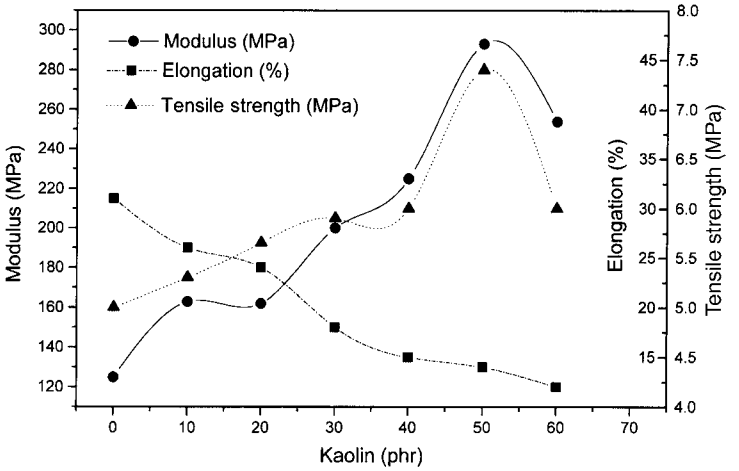

Fig. 15-5 Modulus, ultimate tensile strength, and elongation for thermoplastic starch and its composites with kaolinite. (After Carvalho et al., 2001.)

kaolinite with average particle size of 0.5 μm pre-mixed and processed in an intensive batch mixer at 170°C. Compounds with 0, 10, 20, 30, 40, 50, and 60 parts of kaolinite per hundred parts of thermoplastic starch were prepared. The composite filled with 50 parts per hundred (pph) kaolinite seemed to be the best composition. This showed an increase in the tensile strength from 5 to 7.5 MPa. The modulus of elasticity increased from 120 to 290 MPa and the tensile strain at break decreased from 30% to 14%. Beyond this value the amount of matrix was insufficient to wet kaolinite and the composite became fragile (Fig. 15-5).

Scanning electron microscopy of fractured surfaces revealed a very good dispersion of kaolinite, as there are no smooth areas or large agglomerates. The adhesion between the matrix and kaolinite is also very good and the particles of kaolinite are strongly bonded to the matrix, even after the fracture. Besides the good mechanical properties, the use of these clays also leads to an increase in the water resistance of thermoplastic starch compounds. The presence of kaolinite decreases the water uptake of the composites, this decrease being more pronounced starting at 20 pph (decrease in moisture uptake from 27% to 14% at 100% relative humidity). The observed decrease in glass transition temperature (T_g) is proportional to the amount of kaolinite present in the composites.

The water solubility of starch in kaolinite–starch composite prepared by adding clay to a 3–4% uncooked raw corn starch suspension and subsequent stirring and cooking at 95°C for 30 min was less than 3% at 50°C for 30 min. The clays were distributed well inside the composite and were perfectly coated by starch. When the starch was exposed to high temperature, the solubility increased to 5%. However, crosslinked starch could reduce the solubility even at high temperature. Although the solubility of crosslinked starch increased slightly as temperature increased, the result was only 1.25% at 90°C (Yoon and Deng, 2006).

The influence of different layered compounds (clays) on the properties of starch–clay composites has been described by Wilhelm et al. (2003a, b). Glycerol-plasticized

starch films were modified by addition of various layered compounds as fillers, two being of natural origin (kaolinite as a neutral mineral clay, Ca-hectorite as a cationic exchanger mineral clay) and two synthetic (layered double hydroxide [LDH] as an anionic exchanger and brucite, which has a neutral structure).

The composite materials were prepared by dispersing the layered material in distilled water and adding the dispersion to an aqueous starch dispersion followed by degassing and heating to 100°C in a sealed tube to gelatinize the starch granules. Glycerol (20% w/w, relative to starch on a dry basis) was added to the heated solution and the mixtures were then poured into dishes, allowing solvent evaporation at 40–50°C.

The results obtained in the first investigation showed that the hectorite clay was intercalated in the unplasticized starch matrix, while glycerol–hectorite intercalation was observed in the plasticized films. The unplasticized composite films were very brittle, as expected. A film obtained with 30% w/w of clay showed an increase of more than 70% in the Young's modulus compared to nonreinforced plasticized starch. Both XRD and infrared spectroscopy showed that glycerol can be intercalated into the clay galleries and that there is a possible conformational change of starch in the plasticized starch/clay composite films.

In the subsequent study, it was found that no intercalation took place in presence of kaolinite, LDH, or brucite, while the starch/hectorite composite showed an increase of the interplanar basal distance from 14.4 to 18.3°Å. This basal spacing corresponds to the intercalation of glycerol molecules between the silicate layers, but nonplastiziced starch and/or oxidized starch can also be intercalated into the hectorite galleries. The glycerol intercalation is minimized in plasticized–oxidized starch films where the oxidized starch chains are preferentially intercalated. The storage modulus of the composite materials was higher in the order kaolinite > brucite > hectorite than for LDH starch composites; only the hectorite composites showed an increased T_g.

The rheological properties of composite gels of starch extracted from yam roots and Ca-hectorite were studied in aqueous solutions as a function of hectorite concentration (Wilhelm et al., 2005). The elastic (G') and viscous (G'') moduli of the composite gels were dependent on the clay content. For all samples G' was larger than G''. Composite gels with clay contents of less than 30% exhibited higher G', G'', and viscosity $|\eta_0|$ values compared with pure starch gel, while those with a content of 50% showed lower values. The addition of hectorite significantly inhibited the creeping properties in relation to pure starch at 25°C. However, after heating–cooling cycles between 25 and 85°C, this effect was no longer observable and the composite gel displayed a similar behavior to that of pure starch.

Nanocomposites of glycerol-plasticized starch with untreated montmorillonite and hectorite were examined (Chen and Evans, 2005). The composites were prepared by mixing starch and glycerol at a ratio of 10 : 3 by mass and melt processing to thermoplastic starch on a two-roll mill at 120°C. The clay was added during the processing on the two-roll mill. Organo-treated hectorite and kaolinite were added to produce conventional composites within the same clay volume fraction range for comparison; 10 vol% untreated clay was approximately the maximum loading that this type of TPS could sustain. Unlike natural montmorillonite and hectorite, kaolinite is a nonswelling clay and should produce conventional composites with the starch. TPS/montmorillonite and TPS/hectorite nanocomposites showed an increase of $d001$ from 1.23 to 1.8 nm.

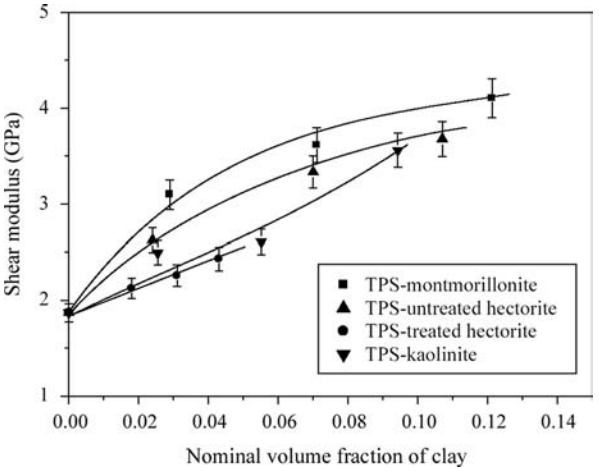

Fig. 15-6 Young's modulus and shear modulus of TPS/clay composites. (After Chen and Evans, 2005.)

The broad 001 peak suggests a wide range of interlayer spacings as a result of the coexistence of intercalation and exfoliation This is further supported by TEM images. However, no changes in the XRD pattern were recorded for the organo-treated hectorite/starch composites, indicating the formation of a conventional composite material.

In all composites, the presence of clay increased both Young's and shear modulus, and the montmorillonite and unmodified hectorite provided significantly more increase than kaolinite, which formed conventional composites with TPS (Fig. 15-6). That the treated-hectorite composites had similar elastic moduli to those prepared from kaolinite, which gives conventional composites, supports the previous observation that they also formed conventional composites. Hectorite particles have a lower aspect ratio and larger surface area than montmorillonite, the former factor tending to give a smaller modulus increase and the latter giving a greater increase. At low clay fractions, montmorillonite provided a higher Young's modulus than the hectorite composite but at higher clay fractions, reinforcement deteriorated. Nevertheless, it is clear that a nanocomposite provides a higher modulus than a conventional composite with the same clay content. Studies of the water absorption of TPS and the TPS/clay nanocomposite containing 6 wt% montmorillonite showed a dramatic softening, swelling, and partial disintegration of the unfilled TPS after immersing in distilled water for 2 hours. However, the nanocomposite remained generally intact after the same immersion conditions. The presence of clay obviously enhances the water resistance of TPS, although exact water absorption data were not obtained.

15.4 BIODEGRADABLE STARCH–POLYESTER NANOCOMPOSITE MATERIALS

There are many sources of biodegradable plastics, from synthetic polymers (polyesters, poly[lactic acid], poly[hydroxybutyrate]s) to natural polymers (starch,

gelatin, chitosan). Synthetic polymers, although having excellent properties, are costly and typically manufactured using nonrenewable petroleum resources. Starch-based thermoplastics, on the other hand, are relatively cheap and, more importantly, are manufactured using renewable sources of raw materials. However, high viscosity and poor melt properties make them difficult to process, and products made from starch are often brittle and water sensitive. To alleviate this problem, starch polymers are often blended with synthetic polymers.

Recent research has indicated that organoclays in combination with biodegradable polyesters show much promise for starch-based polymer nanocomposites in terms of improving their mechanical properties. Organoclay using modifiers consisting of alcohols and hydrogenated tallow, which may be more thermodynamically compatible with the polyester, starch, and an unspecified polyester were blended simultaneously in the twin-screw extruder in order to minimize the time of processing of the starch (McGlashan and Halley, 2003) or in a Haake compounder (Perez et al., 2007). The addition of an organoclay (from 0 to 5 wt%) significantly improved both the processing and tensile properties over the original starch blends; the best results were obtained for 30 wt% starch blends. The increase in tensile strength and Young's modulus is mostly likely due to the enhanced interfacial area of the MMT, providing nanoscale reinforcement of the blend. The tensile strength and Young's modulus of the 30/70 blend nanocomposites were improved by approximately 50% and 200%, respectively. Improvements were also noted for the 50 and 70 wt% starch nanocomposite blends. The incremental improvement in mechanical properties was smaller as the content of starch was increased at clay loading of 1.5%. The same was observed for the higher loading (5 wt%) of MMT. The strain at break was dramatically improved upon the addition of the MMT to the 30 wt% starch (>1500%). The authors suggest that this improvement in elongation could be attributed to the addition of MMT and to better gelatinization and modified crystalline structure of the extrudate. The level of delamination depends on the ratio of starch to polyester and the amount of organoclay added. The crystallization temperature of the nanocomposite blends is significantly lower than that of the base blend. This is probably due to the platelets inhibiting order, and hence crystallization, of the starch and polyester. The effect of organoclay on the melting temperature for any given starch–polyester blend is not significant. The dispersed MMT should make a more tortuous path for the volatile starch plasticizers to escape, which has the twofold effect of lowering the gelatinization temperature of the starch and decreasing the viscosity of the starch–polyester blend. The more amorphous blend deforms plastically rather than failing through brittle fracture. However, the higher the starch loading, then the less the MMT seems to delaminate, and hence the advantage of the large interfacial area of MMT becomes less effective.

The nanocomposite blends were easier to process into films than the base blends using a film-blowing tower. Production of 10 μm-thick film blown on a laboratory film tower and of 30 μm thick films blown on an industrial-scale film blowing unit at production rates typical for low-density polyethylene has been demonstrated.

Starch–polycaprolactone blends filled with Nanomer I.30 E (Nanocor, IL, USA) with loads between 1 and 9 wt% were prepared (Kalambur et al., 2004, 2005). In order to obtain a more "hydrophilic" starch that would form stronger hydrogen

bonds with the clay surface and improve the adhesion, carbonyl or carboxyl groups along the polysaccharide chains were introduced through peroxide-promoted oxidation reactions during a reactive extrusion step. The nanocomposites have much increased solvent resistance properties, most likely due to the increased resistance of the nanocomposite to diffusion. A moderate improvement in tensile strength and much improvement in elongation at break (from 200% to 900%) was achieved.

A more recent study focuses on the improvement of physical and dynamic properties of starch, including thermal plasticity, by blending with polycaprolactone (PCL) (Ikeo et al., 2006). Starch was blended in a first step with glycerin and water to achieve thermal plasticity and improve compatibility with PCL. To improve the compatibility between PCL and TPS, maleic anhydride (MAH) was added to denature the PCL. Using a single-screw extruder, 1 wt% maleic anhydride and 99 wt% PCL were kneaded with 0.3 pph of benzoyl peroxide (BPO) as the

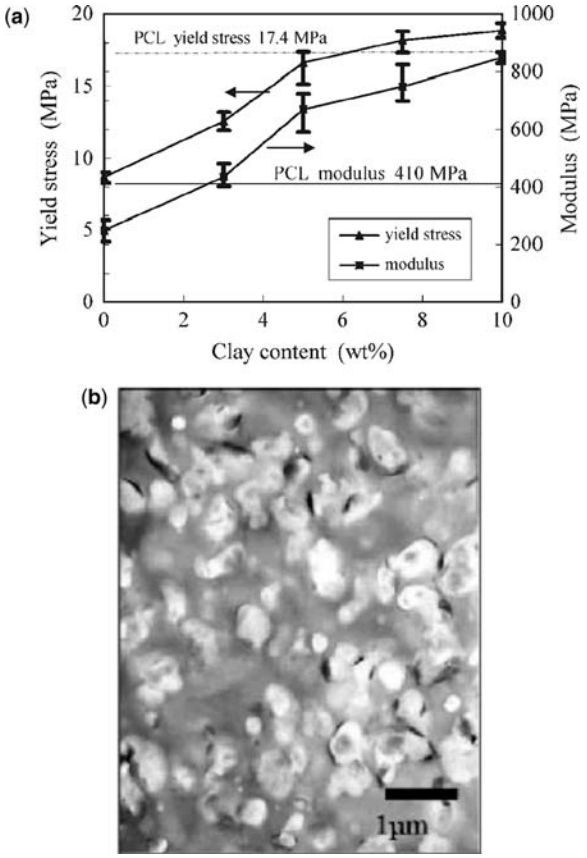

Fig. 15-7 (a) The change of tensile properties for MAHPCL/thermoplastic starch/clay from 50 : 50 : 0 to 50 : 40 : 10 wt%); (b) TEM image of a microtomed sample of MAHPCL/TPS/clay 50/47/3%. (After Ikeo et al., 2006.)

polymerization initiator. Finally, the addition of natural clay (Na-MMT) results in dispersed thermoplastic starch, which improves compatibility with PCL. The clay was dispersed in thermoplastic starch in advance, by kneading in an extruder, to prepare a nanocomposite so as to compensate for degradation of properties caused by adding thermoplastic starch to PCL. Two types of samples were prepared: one containing 10 wt% clay and the other 20 wt%. The clay content in the PCL/thermoplastic starch blends was 3–10 wt%.

According to the result of tensile tests, the strain of PCL/thermoplastic starch/clay blends is extremely low at around 3%, while that of MAHPCL/thermoplastic starch/clay exceeds 500% (Fig. 15-7). As can be seen from this result, both strain and yield strength were significantly improved after adding maleic anhydride to PCL. The blends with 5 wt% or higher clay content have modulus and yield strength equal to or higher than PCL alone. The blend with 10 wt% or higher clay content shows modulus two times or higher that of PCL alone; hence adding maleic anhydride and clay to the PCL/thermoplastic starch blend significantly improved its properties. The addition of clay is believed to have increased the viscosity of the thermoplastic starch phase close to that of PCL, which resulted in improved compatibility.

Novel biodegradable starch/clay/polyester (Ecoflex®, BASF) nanocomposite films, to be used as food packaging, were obtained by homogeneously dispersing native Na-MMT nanoparticles in different starch-based materials via polymer melt processing techniques (Avella et al., 2005). For starch/clay material, the results show good intercalation of the polymeric phase into clay interlayer galleries, together with an increase in mechanical parameters, such as modulus and tensile strength. In the case of starch/polyester/clay, a separation of the polyester phase was observed.

15.5 DISCUSSION AND CONCLUSION

Homogeneous incorporation of clay particles into a starch matrix on a true nano scale has proved possible. The stiffness, the strength, and the toughness of the nanocomposite materials are improved even at very low loadings of clay (2–4%) if the platelets are completely exfoliated and can be adjusted by varying the water content (Fischer et al., 2001; Dean et al., 2007). Starch/clay nanocomposites can be formed when complete TPS (verification of the absence of crystals is essential) is used and enough plasticizer is present in a combination of glycerol/sorbitol and water and when sufficient shear force is applied, preferably in a twin-screw extruder. In addition, knowledge of the degree of retrogradation is essential for eventually marketable products in consumer applications.

The addition of clay during processing supports and intensifies the destructurization of starch, providing a means of easier processing (lower extrusion temperature and less use of processing agents). The starch/clay nanocomposite films show a very strong decrease in hydrophilicity, no dramatic softening, swelling, and partial disintegration, unlike unfilled TPS after immersing in distilled water.

However, if no complete exfoliation has been achieved, it is very difficult to judge the effect of the reinforcing minerals. When (some) clusters of aggregated clay

particles are present within the samples they can influence the overall mechanical properties and dominate the deformation behavior. In such cases only minor improvements can be expected and such are reported. Starch/clay nanocomposites can only be formed if the starch has been totally destructurized into a homogeneous thermoplastic material to ensure a homogeneous distribution of the nanoparticles. The destructurization always occurs above the glass transition temperature (T_g) and shifts the final T_g to lower temperatures. TPS with a plasticizer content below 30% has a T_g above room temperature and thus remains brittle. The modulus change is reversed proportionally with the quantity of plasticizer (or water) and therefore the mechanical properties will change when the relative humidity of the atmosphere changes. The modulus determined from test samples will be substantially lower on humid days compared with values obtained on dry days. Clay delays the brittleness by delaying the migration of plasticizer (moisture) to the surroundings but it cannot prevent the sample eventually becoming brittle in time.

Water stability can only be obtained in completely retrogradated samples, conditioned at high relative humidities RH $>$ 90%. It is known that samples conditioned at 50% RH will not be stable over time because of slow recrystallization/retrogradation.

Results from different research groups cannot always be compared due to the different sample preparation steps employed. It would be useful to agree some standard on how to prepare samples for analysis.

When comparing different clays it is seen that the actions of untreated montmorillonite and hectorite are very similar but are fundamentally different from that of fillers such as kaolinite and organo-treated hectorite and kaolinite. Both are nonswelling clays in aqueous and plasticizer environments and produce conventional (micro)-composites with the starch. The adhesion between the matrix and filler particles is in general very good and the particles are strongly bonded to the matrix, even after fracture.

When combining starch with biodegradable polyesters a choice has to made of which phase should be reinforced by the clay particles and consequently the means of compatibilization to be used. Mostly, organoclay using modifiers consisting of amines substituted with alcohols and hydrogenated tallow are used, which are more thermodynamically compatible with the polyester, The addition of an organoclay (from 0 to 5 wt%) to starch/polyester blends may offer advantages with respect to the processing and tensile properties over the original starch blends; the increase in tensile strength and Young's modulus is most likely due to the enhanced interfacial area.

Because of water sensitivity, samples stored under normal ambient conditions will always eventually become brittle. Addition of biodegradable polyesters to starch–clay composites is always necessary for applications in packaging, whether in blown films or molded products. In these kinds of applications it then becomes questionable whether clay makes a large difference when polyesters are used in large quantities. More research is needed to discover whether the use of starch–clay nanocomposites might be effective in reducing the amount of polyester and thus help products made from these blends to become eventually more compatible with conventional plastics.

REFERENCES

Avella M, De Vlieger JJ, Errico ME, Fischer S, Vacca P, Volpe MG. 2005. Biodegradable starch/clay nanocomposite films for food packaging applications. *Food Chemistry* 93:467–474.

Bagdi K, Müller P, Pukánszky B. 2006. Thermoplastic starch/layered silicate composites: structure, interaction, properties. *Composites Interfaces* 13:1–17.

Carvalho AJF, Curvelo AAS, Agnelli JAM. 2001. A first insight on composites of thermoplastic starch and kaolinite. *Carbohydrate Polymers* 45:189–194.

Chen B, Evans JRG. 2005. Thermoplastic starch-clay nanocomposites and their characteristics. *Carbohydrate Polymers* 51:455–463.

Chiou BS, Lee E, Glenn GM, Orts WJ. 2005. Rheology of starch–clay nanocomposites. *Carbohydrate Polymers* 59:467–475.

Dean K, Yu L, Wu DY. 2007. Preparation and characterisation of melt-extruded thermoplastic starch/clay nanocomposites. *Composites Science and Technology* 67:413–421.

Fischer S, De Vlieger J, Kock T, Batenburg L, Fischer H. 2001. "Green" nano-composite materials—new possibilities for bioplastics. *Material Research Society Symposium Proceedings* 661:KK221–KK226.

Huang M, Yu J. 2006. Structure and properties of thermoplastic corn starch/montmorillonite biodegradable composites. *Journal of Applied Polymer Science* 99:170–176.

Huang MF, Yu JG, Ma XF. 2004. Studies on the properties of montmorillonite-reinforced thermoplastic starch composites. *Polymer* 45:7017–7023.

Huang MF, Yu JG, Ma XF, Jin P. 2005a. High performance biodegradable thermoplastic starch-ENMT thermoplastics. *Polymer* 46:3157–3162.

Huang MF, Yu JG, Ma XF. 2005b. Preparation of the thermoplastic starch/montmorillonite nanocomposites by melt-intercalation. *Chinese Chemical Letters* 16:561–564.

Huang M, Yu J, Ma X. 2006. High mechanical performance MMT-urea and formamide-plasticized thermoplastic cornstarch biodegradable nanocomposites. *Carbohydrate Polymers* 63:393–399.

Ikeo Y, Aoki K, Kishi H, Matsuda S, Murakami A. 2006. Nano clay reinforced biodegradable plastics of PCL starch blends. *Polymers for Advanced Technologies* 17:940–944.

Kalambur SB, Rizvi SSH. 2004. Starch-based nanocompositesby reactive extrusion processing. *Polymer International* 53:1413–1416.

Kalambur SB, Rizvi SSH. 2005. Biodegradable and functionally superior starch-polyester nanocomposites from reactive extrusion. *Journal of Applied Polymer Science* 96:1072–1082.

Kampeerapappun P, Aht-ong D, Pentrakoon D, Srikulkit K. 2007. Preparation of cassava starch/montmorillonite composite film. *Carbohydrate Polymers* 67:155–163.

Kudryavtsev YV, Govorun EN, Litmanovich AD, Fischer H. 2004. Polymer melt intercalation in clay modified by diblock copolymers. *Macromolecular Theory and Simulations* 13:392–399.

Ma X, Yu J, Wang N. 2007. Production of thermoplastic starch/MMt-sorbitol nanocomposites by dual-melt extrusion processing. *Macromolecular Material Engineering* 292:723–728

McGlashan SA, Halley PJ. 2003. Preparation and characterisation of biodegradable starch-based nanocomposite materials. *Polymer International* 52:1767–1773.

Pandey JK, Singh RP. 2005. Green nanocomposites from renewable resources: Effect of plasticizer on the structure and material properties of clay-filled starch. *Starch/Staerke* 57:8–15.

Park HM, Li X, Jin CZ, Park CY, Cho WJ, Ha CS. 2002. Preparation and properties of biodegradable thermoplastic starch/clay hybrids. *Macromolecular Material Engineering* 287:553–558.

Park HM, Lee WK, Park CY, Cho WJ, Ha CS. 2003. Environmentally friendly polymer hybrids, Part 1. Mechanical, thermal, and barrier properties of thermoplastic starch/clay nanocomposites. *Journal of Materials Science* 38:909–915.

Pérez, CJ, Alvarez, VA, Mondragón I, Vázquez A. 2007. Mechanical properties of layered silicate/starch polycaprolactone blend nanocomposites. *Polymer International* 56:686–693.

Qiao X, Jiang W, Sun K. 2005. Reinforced thermoplastic acetylated starch with layered silicates. *Starch/Staerke* 57:581–586.

Wilhelm HM, Sierakowski MR, Souza GP, Wypych F. 2003a. Starch films reinforced with mineral clay. *Carbohydrate Polymers* 52:101–110.

Wilhelm HM, Sierakowski MR, Souza GP, Wypych F. 2003b. The influence of layered compounds on the properties of starch/layered compound composites. *Polymer International* 52:1035–1044.

Wilhelm HM, Sierakowski MR, Reicher F, Wypych F, Souza GP. 2005. Dynamic rheological properties of yam starch/hectorite composite gels. *Polymer International* 54:814–822.

Yang KK, Wang XL, Wang YZ. 2007. Progress in nanocomposite biodegradable polymer. *Journal of Industrial Engineering Chemistry* 13:485–500.

Yoon SY, Deng Y. 2006. Clay–starch composites and their application in papermaking. *Journal of Applied Polymer Science* 100:1032–1038.

Yu L, Petinakis S, Dean K., Bilyk A., Dongyang W. 2007. Green polymer blends and composites from renewable resources. *Macromolecular Symposium* 249:535–539.

CHAPTER 16

Polylactide-Based Nanocomposites

SUPRAKAS SINHA RAY and JAMES RAMONTJA

National Centre for Nano-Structured Materials, Council for Scientific and Industrial Research, Pretoria 0001, Republic of South Africa

16.1 INTRODUCTION

In recent years, biodegradable polymers from renewable resources have attracted great research attention (Ikada and Tsuji, 2000). Biodegradable polymers are defined as those that undergo microbially induced chain scission leading to mineralization (Sinha Ray and Bousmina, 2005). Specific conditions in term of pH, humidity, oxygenation and the presence of some metals are required to ensure the biodegradation of such polymers. Renewable sources of polymeric materials offer an alternative for maintaining sustainable development of economically and ecologically attractive technology. Innovations in the development of materials from biodegradable

Biodegradable Polymer Blends and Composites from Renewable Resources. Edited by Long Yu

polymers, the preservation of fossil-based raw materials, complete biological degradability, reduction in the volume of garbage and compostability in the natural cycle, protection of the climate through the reduction of carbon dioxide released, as well as the possible application of agriculture resources for the production of green materials are some of the reasons why such materials have attracted academic and industrial interest.

One of the most promising polymers in this direction is polylactide (PLA) because it is made wholly from agricultural products and is readily biodegradable (Gruber and Brien, 2002). PLA is not a new polymer and has been the subject of many investigations for over a century. In 1845, Pelouze condensed lactic acid by distillation of water to form low-molecular-weight PLA and the cyclic dimer of lactic acid, known as lactide (Pelouze, 1845). About a half-century later, an attempt was made by Bischoff and Walden to polymerize lactide to PLA (Bischoff and Walden, 1894); however, the method was unsuitable for practical use (Watson, 1948). In 1948, Watson published a review on the possible uses of PLA for coatings and as a constituent in resins. Despite being known for over 100 years, PLA has not been commercially viable or practically useful, although it was described as having potential as a commodity plastic (Lipinsky and Sinclair, 1986). However, recent developments in the manufacturing of the monomer economically from agricultural products have placed this material at the forefront of the emerging biodegradable plastics industries (Vink et al., 2003).

In recent years, high-molecular-weight PLA has generally been produced by the ring-opening polymerization of the lactide monomer. The conversion of lactide to high-molecular-weight polylactide is achieved by two routes: (i) direct condensation, which involves solvents under high vacuum, and (ii) formation of the cyclic dimer intermediate (lactide), which is solvent free. Until 1990, the monomer lactide was produced commercially by fermentation of petrochemical feedstocks. The monomer produced by this route is an optically inactive racemic mixture of L- and D-enantiomers. Today the most popular route is fermentation in which corn starch is converted into lactide monomer by bacterial fermentation (Drumright and Gruber, 2000).

Recently, Cargill-Dow used a solvent-free process and a novel distillation process to produce a range of PLAs (Lunt, 1998; Drumright and Gruber, 2000). The essential novelty of this process lies in its ability to go from lactic acid to a low-molecular-weight poly(lactic acid), followed by controlled depolymerization to produce the cyclic dimer, commonly referred to as lactide. This lactide is maintained in liquid form and purified by distillation. Catalytic ring-opening polymerization of the lactide intermediate results in the production of PLAs with controlled molecular weights. The process is continuous with no need to separate the intermediate lactide.

In contrast, Mitsui Toatsu (now, Mitsui Chemicals) utilizes a solvent-based process in which a high-molecular-weight PLA is produced by the direct condensation using azeotropic distillation to continuously remove the condensation water (Enomoto et al., 1994). Commercially available PLA grades are copolymers of poly(L-lactide) with *meso*-lactide or D-lactide. The amount of the D enantiomer is

TABLE 16-1 Physical Properties of PLA

Property	Typical Value
Molecular weight (kg/mol)	100–300
Glass transition temperature, T_g (°C)	55–70
Melting temperature, T_m (°C)	130–215
Heat of melting, ΔH_m (J/g)	8.1–93.1
Degree of crystallinity, X (%)	10–40
Surface energy (dynes)	38
Solubility parameter, δ $(J/ml)^{1/2}$	19–20.5
Density, ρ (kg/m^3)	1.25
Melt flow rate, MRF (g/10 min)	2–20
Permeability of O_2 and CO_2 (fmol m^{-1} s^{-1} Pa^{-1})	4.25 and 23.2
Tensile modulus, E (GPa)	1.9–4.1
Yield strength (MPa)	70/53
Strength at break (MPa)	66/44
Flexural strength (MPa)	119/88
Elongation at break (%)	100–180
Notched Izod impact strength (J/m)	66/18
Decomposition temperature (K)	500–600

known to affect the properties of PLA—melting temperature, degree of crystallinity, and so on.

PLA has a balance of mechanical properties, thermal plasticity, and biodegradability, and is readily fabricated; it is thus a promising polymer for various end-uses (Fang and Hanna, 1999; Gu et al., 1992). Various properties of PLA are summarized in Table 16-1. Even when burned, it produces no nitrogen oxide gases and only one-third of the combustion heat generated by polyolefins; it does not damage the incinerator and provides significant energy savings.

The increasing appreciation of the various intrinsic properties of PLA, coupled with knowledge of how such properties can be improved to achieve compatibility with thermoplastics processing, manufacturing, and end-use requirements, has fuelled technological and commercial interest in PLA.

Over the last few years, a wealth of investigations have been undertaken to enhance the mechanical properties and the impact resistance of PLA. It can therefore compete with other low-cost biodegradable/biocompatible or commodity polymers. These efforts have made use of biodegradable and nonbiodegradable fillers and plasticizers or blending of PLA with other polymers (Martin and Averous, 2001).

In recent years the nanoscale, and the associated excitement surrounding nanoscience and technology, has afforded unique opportunities to create revolutionary material combinations. These new materials promise the circumvention of classical material performance trade-offs by accessing new properties and exploiting unique synergisms between constituents that occur only when the length scale of the morphology and the critical length associated with the fundamental physics of a given property coincide.

Nanostructured materials or nanocomposites based on polymers have been an area of intense industrial and academic research over the past one and a half decades (LeBaron et al., 1999; Alexander and Doubis, 2000; Zanetti et al., 2000; Biswas and Sinha Ray, 2001; Sinha Ray and Okamoto, 2003a). In principle, nanocomposites are an extreme case of composite materials in which interfacial interactions between two phases are maximized. In the literature, the term nanocomposite is generally used for polymers with submicrometer dispersions. In polymer-based nanocomposites, nanometer-sized particles of inorganic or organic-materials are homogeneously dispersed as separate particles in a polymer matrix. This is one way of characterizing this type of material. There is, in fact, a wide variety of nanoparticles and of ways to differentiate them and to classify them by the number of dimensions they possess. Their shape varies and includes: (i) needlelike or tubelike structures regarded as one-dimensional particles, for example, inorganic nanotubes, carbon nanotubes, or sepiolites; (ii) two-dimensional platelet structures, for example, layered silicates; and (iii) spheroidal three-dimensional structures, for example, silica or zinc oxide.

The main objective of this chapter is to provide a snapshot of the rapidly developing field of nanocomposite materials based on PLA. To date, various types of nanoreinforcements such as nanoclay, cellulose nanowhiskers, ultrafine layered titanate, nanoalumina, and carbon nanotubes (Mohanty et al., 2003; Nazhat et al., 2001; Hiroi et al., 2004; Nishida et al., 2005; Mark 2006; Kim et al., 2006). have been used for the preparation of nanocomposites with PLA. Progress in each particular system is discussed chronologically starting from the pioneering works. Various physicochemical characterizations and improved mechanical properties are summarized. Ongoing developments and promising avenues are also discussed. Finally, possible applications and prospect for nanocomposites based on PLA are mentioned.

16.2 PLA NANOCOMPOSITES BASED ON CLAY

Polymer nanocomposites based on clay minerals have attracted great interest from researchers in recent times, both in industry and in academia, because they often exhibit concurrent improvements in properties over the neat polymers. These improvements can include high moduli, increased strength and heat resistance, decreased gas permeability and flammability, and increased degradability of biodegradable polymers (LeBaron et al., 1999; Alexander and Doubis, 2000; Zanetti et al., 2000; Biswas and Sinha Ray, 2001; Sinha Ray and Okamoto, 2003a). On the other hand, these materials have also been demonstrated to be unique model systems for the study of the structure and dynamics of polymers in confined environments (Sinha Ray, 2006).

16.2.1 Structure and Properties of Clay

The commonly used clay minerals for the preparation of polymer/clay nanocomposites belong to the same general family of 2 : 1 layered silicates or phyllosilicates (Brindly and Brown, 1980; Sinha Ray and Okamoto, 2003a). Their crystal structure

consists of layers made up of two tetrahedrally coordinated silicon atoms fused to an edge-shared octahedral sheet of either aluminum or magnesium hydroxide. The layer thickness is around 1 nm, and the lateral dimensions of these layers may vary from 30 nm to several micrometers or larger, depending on the particular clay minerals. Stacking of the layers leads to a regular van der Waals gap between the layers called the interlayer or gallery. Isomorphic substitution within the layers (for example, Al^{3+} replaced by Mg^{2+} or Fe^{2+}, or Mg^{2+} replaced by Li^{+}) generates negative charges that are counterbalanced by alkali and alkaline earth cations situated inside the galleries. This type of clay mineral is characterized by a moderate surface charge, known as the cation exchange capacity (CEC), and generally expressed as mequiv/100 g. This charge is not locally constant but varies from layer to layer, and must be considered as an average value over the whole crystal.

Montmorillonite (MMT), hectorite, and saponite are the most commonly used clay minerals for the preparation of nanocomposites. Clay minerals generally have two types of structure: tetrahedral-substituted and octahedral-substituted. In the case of tetrahedrally-substituted clay minerals, the negative charge is located on the surface of the silicate layers, and hence the polymer matrices can interact more readily with these than with octahedrally-substituted material.

Two particular characteristics of clay minerals are generally considered in the preparation of clay-containing polymer nanocomposites. The first is the ability of the silicate particles to disperse into individual layers. The second characteristic is the ability to modify their surface chemistry through ion-exchange reactions with organic and inorganic cations. These two characteristics are, of course, interrelated since the degree of dispersion of silicate layers in a particular polymer matrix depends on the interlayer cation.

Pristine layered silicates usually contain hydrated Na^{+} or K^{+} ions (Sinha Ray and Okamoto, 2003a; Sinha Ray and Bousmina, 2005). Obviously, in this pristine state, layered silicates are only miscible with hydrophilic polymers. To render clay particles miscible with PLA matrix, one must convert the normally hydrophilic silicate surface into an organophilic one, making possible the intercalation of PLA chains into the silicate galleries. Generally, this can be done by ion-exchange reactions with cationic surfactants including primary, secondary, tertiary, and quaternary alkylammonium or alkylphosphonium cations. Alkylammonium or alkylphosphonium cations in the organosilicates lower the surface energy of the inorganic host and improve the wetting characteristics of the polymer matrix, and the result is a larger interlayer spacing. Additionally, the alkylammonium or alkylphosphonium cations can provide functional groups that can react with the polymer matrix, or in some cases initiate the polymerization of monomers to improve the adhesion between the inorganic and the polymer matrix.

16.2.2 Preparation and Characterization of PLA/Clay Nanocomposites

Ogata and co-workers first reported the preparation of PLA/organoclay blends by dissolving the PLA in hot chloroform in the presence of dimethyldistearylammonium

modified MMT (2C18MMT) (Ogata et al., 1997). In the case of PLA/MMT composites, wide-angle X-ray diffraction (WXRD) and small-angle X-ray scattering (SAXS) results showed that the silicate layers forming the clay could not be intercalated in the PLA/MMT blends prepared by the solvent-casting method. In other words, the clay existed in the form of tactoids, consisting of several stacked silicate monolayers. These tactoids are responsible for the formation of particular geometrical structures in the blends, which leads to the formation of superstructures in the thickness of the blended film. This kind of structural feature increases the Young's modulus of the hybrid. Then Bandyopadhyay et al. (1999) reported the preparation of intercalated PLA/organoclay nanocomposites with much improved mechanical and thermal properties. Two different kinds of clay, fluorohectorite (FH) and MMT, both modified with dioctadecyltrimethyl ammonium cation, were used for the preparation of nanocomposites with PLA.

Sinha Ray and co-workers used the same melt intercalation technique for the preparation of intercalated PLA/organoclay nanocomposites (Sinha Ray et al., 2002a,b). XRD patterns and TEM observations clearly established that the silicate layers of the clay were intercalated and randomly distributed in the PLA matrix (see Fig. 16-1). Incorporation of a very small amount of oligo-PCL as a compatibilizer in the nanocomposites led to a better parallel stacking of the silicate layers, and

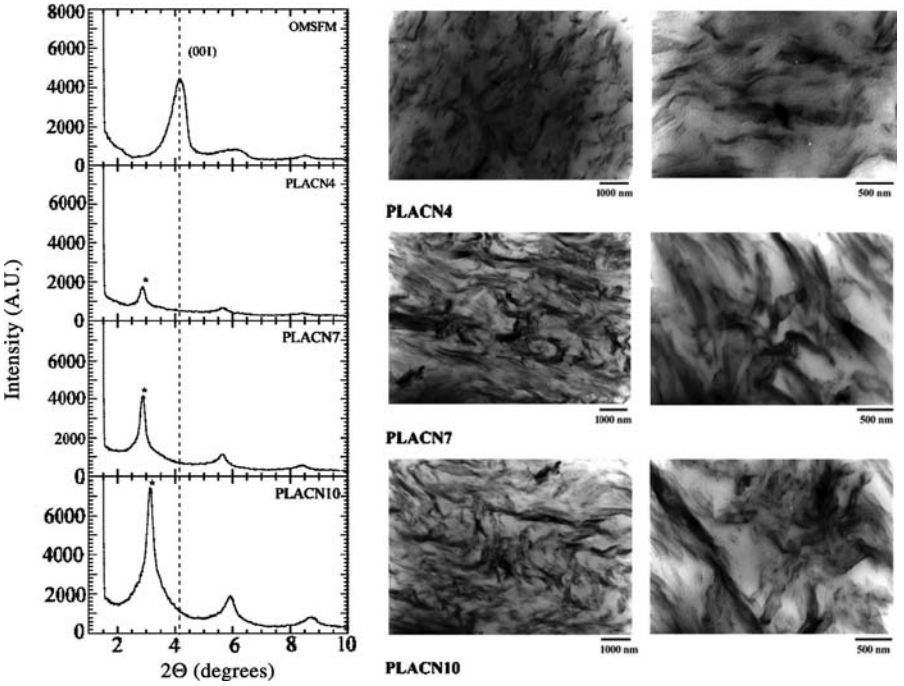

Fig. 16-1 XRD patterns and bright-field images of PLA nanocomposites prepared with organically modified synthetic fluorine mica. The number indicates amount of organoclay loading.

also to much stronger flocculation due to the hydroxylated edge–edge interaction of the silicate layers. Owing to the interaction between clay platelets and the PLA matrix in the presence of a very small amount of o-PCL, the strength of the disk–disk interaction plays an important role in determining the stability of the clay particles, and hence the enhancement of mechanical properties of such nanocomposites.

In subsequent research, Sinha Ray and co-workers (Sinha Ray et al., 2002c, 2003a,b,c,d) prepared PLA nanocomposites with organically modified synthetic fluorine mica (OMSFM). For the characterization of structure and morphology of prepared nanocomposites they first used XRD and conventional TEM (CTEM), and high resolution TEM (HRTEM), to examine the final structure of the PLACNs (PLACN is abbreviation of PLA Nanocomposites). In their further study Sinha Ray et al., 2003c) prepared a series of PLA-based nanostructured materials with various types of organoclays to investigate the effect of organic modification on the morphology, properties, and degradability of the final nanocomposites.

Maiti and co-workers prepared a series of PLA-based nanostructured materials with three different types of pristine clays—saponite (SAP), MMT, and synthetic mica (SM)—and each was modified with alkylphosphonium salts having different chain lengths. In their work, they first tried to determine the effect of varying the chain length of the alkylphosphonium modifier on the properties of organoclay, and how the various clays behave with the same organic modifier. They also studied the effects of dispersion, intercalation, and the aspect ratio of the clay particles on the properties of PLA (Maiti et al., 2002).

Paul et al. (2003) used an in-situ intercalative method for the preparation of exfoliated PLA/clay nanocomposites. They used two different kinds of organoclays (C30B and C25A, commercial names; Southern Clay Products) for the preparation of nanocomposites with PLA. In a typical synthetic procedure, the clay was first dried overnight at 70°C in a ventilated oven, and then, at the same temperature under reduced pressure, directly in the flame-dried polymerization vial for 3.5 h. A 0.025 molar solution of L-lactide in dried tetrahydrofuran (THF) was then transferred under nitrogen to the polymerization vial and the solvent was eliminated under reduced pressure. Polymerizations were conducted in bulk at 120°C for 48 h, after 1 h of clay swelling in the monomer melt. When C30B was used, the polymerization was co-initiated by a molar equivalent of $AlEt_3$, with respect to the hydroxyl groups borne by the ammonium cations of the filler, in order to form aluminum alkoxide active species, and was added before the L,L-lactide. $Sn(Oct)_2$ (monomer/$Sn(Oct)_2 = 300$) was used to catalyze the polymerization of L,L-lactide in the presence of C25A. The same group (Paul et al., 2003) also reported the preparation of plasticized PLA/MMT nanocomposites by melt intercalation technique. The organoclay used was MMT modified with bis-(2-hydroxyethyl) methyl (hydrogenated tallow alkyl) ammonium cations. XRD analyses confirmed the formation of intercalated nanocomposites.

Chang et al. (2003a) reported the preparation of PLA-based nanocomposites with three different kinds of organoclays a via solution intercalation method. They used *N*,*N*′-dimethylacetamide (DMA) for the preparation of nanocomposites. XRD patterns indicate the formation of intercalated nanocomposites whatever the organoclay. TEM images proved that most of the clay layers were dispersed

homogeneously in the PLA matrix, although some clusters or agglomerated particles were also detected.

Krikorian and co-workers explored the effect of compatibility of different organic modifiers on the overall extent of dispersion of layered silicate layers in a PLA matrix (Krikorian and Pochan, 2003). Three different types of commercially available organoclays were used as a reinforcement phase. Nanocomposites were prepared using the solution-intercalation film-casting technique.

Lee et al. (2003) prepared PLA/MMT nanocomposite for the purpose of tailoring mechanical stiffness of PLA porous scaffold systems. They used a salt leaching/gas foaming method for the preparation of the nanocomposite scaffold. A viscous solution with a concentration of 0.1 g/ml was prepared by dissolving PLA polymer in chloroform. NH_4HCO_3/NaCl salt particles sieved in the range of 150–300 μm and dimethyl dehydrogenated tallow ammonium modified MMT (2M2HT-MMT) clays were added to the PLA solution and thoroughly mixed. The amount of the 2M2HT-MMT clay was 2.24, 3.58, and 5.79 vol% relative to PLA.

The paste mixture of polymer/salts/solvent was then cast into a special device equipped with a glass slide as a sheet model. The cast film was obtained after being air-dried under atmospheric pressure for 2 h. When the film became semisolid, a two-step salt leaching was performed. The film was first immersed in a 90°C hot water bath to leach out the NH_4HCO_3 particles, concomitantly generating gaseous ammonia and carbon dioxide in the polymer matrix. When no gas bubbles were generated, the film was subsequently immersed into another beaker containing hot water (~60°C), and kept there for 30 min to leach out the remaining NaCl particles. It was finally, freeze dried for two days.

From the XRD patterns, it was seen that pure 2M2HT-MMT demonstrated a sharp peak at $2\theta = 3.76^\circ$ and this peak was not observed in the case of the nanocomposite, indicating the formation of exfoliated PLA/2M2HT-MMT nanocomposite, but the authors did not report any TEM observations. Recently, various authors have reported the preparation of PLA/clay nanocomposites using different synthetic routes (Kramschuster et al., 2004; Nam et al., 2004; Ninomiya et al., 2004).

16.3 PLA NANOCOMPOSITES BASED ON CARBON NANOTUBES

In the past decade, carbon nanotubes (CNTs) have attracted more and more interest from both scientists and engineers because of their extraordinarily high strength and high modulus (the strongest material known nowadays), their excellent electrical conductivity along with their important thermal conductivity and stability, and their low density associated with their high aspect ratio and one-dimensional tubular structure, and hence their tremendous potential in applications such as nanoengineering and bionanotechnology (Thostenson et al., 2001; Zhang et al., 2003; Andrews and Weisenberger, 2004; Xie et al., 2005; Awasthi et al., 2005; Sinha Ray et al., 2006; Banerjee et al., 2005; Miyagawa et al., 2005; Fernando et al., 2005; Yang et al., 2005; Kim et al., 2005; Vaudreuil et al., 2007; Shi et al. 2005, 2006; Baibarac and Gomez-Romero, 2006; Cui et al., 2006; Zhang et al., 2006).

CNTs are giant fullerenes. A fullerene, by definition, is a closed, convex cage molecule containing only hexagonal and pentagonal faces. CNTs have many structures, differencing in length, thickness, types of spiral, and number of layers, although they are formed from essentially the same graphite sheet. Graphite has three-coordinate sp^2 carbons forming planar sheets, whose motif is the flat six-membered benzene ring. In fullerene the three-coordinate carbon atoms tile the spherical or nearly spherical surfaces, the best known example being C_{60} with a truncated icosahedral structure formed by 12 pentagonal rings and 20 hexagonal rings. There are two main types of CNTs: single-walled CNTs (SWCNTs) and multi-walled CNTs (MWCNTs).

Theoretically, it is possible to construct an sp^2-hybrized carbon tubule by rolling up a hexagonal graphene sheet. This leads to two different types of arrangements such as "nonchiral" and "chiral". In the nonchiral arrangements, the honeycomb lattices, located at the top and bottom of the tube, are always parallel to the tube axis and these configurations are known as armchair and zig-zag. In the armchair structure, two C–C bonds on opposite sides of each hexagon are perpendicular to the tube axis, whereas in the zig-zag arrangement, these bonds are parallel to the tube axis. All other conformations in which the C–C bonds lie at an angle to the tube axis are known as chiral or helical structures.

Moon and co-workers prepared PLA/MWCNT nanocomposites by the solvent casting method (Moon et al., 2005). They used two different methods for the synthesis of nanocomposites: (i) A 10 wt% solution of PLA in chloroform was prepared, which was then combined with previously dispersed MWCNTs in chloroform and the whole mixture was sonicated for 6 h. Subsequently, the mixture was poured into Teflon dishes and dried at room temperature for one week and then sample was vacuum-dried at 80°C for 8 h. (ii) The As-cast composite films from method 1 were folded and broken into pieces of 0.5–1.0 cm^2 and stacked between two metal plates. This stack was then hot pressed at 200°C and 150 kgf/cm^2 for 15 min. As a result 100–200 μm thick films were obtained. Transmission electron microscopic analysis shows uniform dispersion of MWCNTs into the PLA matrix. This uniform dispersion of MWCNTs changes the physical properties of the pure polymer.

Chen et al. (2005) synthesized PLA/CNT nanocomposites using a "grafting to" technique. To elucidate the effect of molecular weight on the properties of final nanocomposites, they used PLA of three different molecular weights. They first oxidized MWCNTs by acid treatment. In a typical procedure, a 500 ml flask charged with 2.5 g of the crude MWCNTs and 200 ml of 60% HNO_3 aqueous solution was sonicated in a bath (28 kHz) for 30 min. The mixture was then stirred for 12 h under reflux. After the solution was cooled to room temperature, it was diluted with 400 ml of deionized water and vacuum-filtered through a 0.22 μm polycarbonate membrane. The solid was washed with deionized water until the pH of the filtrate reached approximately to 7. The solid was then dried under vacuum for 12 h at 60°C to yield 1.5 g of the carboxylic-acid-functionalized MWCNT (MWCNT-COOH).

For the preparation of nanocomposites, MWCNT-COOH was first reacted with excess thionyl chloride ($SOCl_2$) for 24 h under reflux, and then the residual $SOCl_2$ was removed by reduced-pressure distillation to yield the acyl-chloride-functionalized

MWCNT (MWCNT-COCL). The MWCNT-COCl was added to chloroform, and the reactor was then immersed in an oil bath at 70°C with methanol stirring for 1 h to remove the solvent. The reaction was allowed to proceed for 24 h at 180°C and 1 atm. The resulting reaction medium was dissolved in excess chloroform and vacuum-filtered three times through 0.22 μm polycarbonate membrane to yield the MWCNT-*g*-PLLA hybrid by filtering the chloroform-soluble substances such as the unbound PLLA. The MWCNT-*g*-L-PLA hybrids were prepared using the PLLAs with three different molecular weights of 1000 g/mol, 3000 g/mol, 11,000 g/mol, and 15,000 g/mol, which are represented as MWCNT-*g*-PLLA1, MWCNT-g-PLLA2, MWCNT-*g*-PLLA3, and MWCNT-*g*-PLLA4, respectively.

Various techniques were used for the characterization of the prepared nanocomposite samples. The composition of the resulting MWCNT-*g*-PLLA nanocomposites was confirmed by FTIR. The results showed the retention of PLLA even after extensive washing with a good solvent for the PLLA. Raman analysis revealed that the D- and G-bands of the MWCNT at 1287 and 1598 cm^{-1} for both MWCNT-COOH and MWCNT-*g*-PLLA2, which were attributed to the defects and disorder-induced peaks and tangential-mode peaks. The peak intensity of the MWCNT-*g*-PLLA2 was much weaker than that of the MWCNT-COOH, which means that the characteristic absorption peaks were strongly attenuated due to the grafted PLLA.

Thermogravimetric analysis (TGA) and TEM observations indicated that the amount of grafted PLLA and its morphology depended strongly on the molecular weight of the PLLA. As the molecular weight of the PLLA increased from 1000 to 3000, the PLLA coating on the MWCNT became thicker and more uniform. When the molecular weight of the PLLA was increased further to 11,000 and 15,000, the surface of the MWCNT was not covered wholly but was sparsely stained with the PLLA. The grafted PLLA formed bolds exhibiting a morphology that was like a squid leg. The MWCNT-*g*-PLLA prepared using PLLA with molecular weight of 3000 was more readily dispersed in inorganic solvent such as chloroform and *N,N*-dimethylformamide (DMF) than that obtained using other PLLAs. This was attributed to the higher PLLA content and the smaller area of the MWCNT surface. More recently, Song et al. (2007) reported the one-step synthesis of PLA-*g*-MWCNT nanocomposite.

16.4 PLA NANOCOMPOSITES BASED ON VARIOUS OTHER NANOFILLERS

Hiroi and co-workers prepared PLA/organically modified layered titanate nanocomposites by a melt-extrusion method (Hiroi et al., 2004). For the preparation of organically modified layered titanate, a blend of K_2CO_3 (304 g), Li_2CO_3 (54 g), TiO_2 (762 g), and KCl (136 g) was mixed intimately and heated at 1020°C for 4 h in an electric furnace. After cooling, the powder was dispersed to a 5 wt% water slurry and 10 wt% of H_2SO_4 water solution was added while agitating for 2 h until a pH of 7 was reached.

This slurry was filtered off and rinsed with water, and then dried at 110°C. After this, it was heated at 600°C for more than 3 h in an electric furnace. The white powder

obtained was $K_{0.7}Ti_{1.73}Li_{0.27}O_{3.95}$ with an average particle size of 32 mm. $K_{0.7}Ti_{1.73}Li_{0.27}O_{3.95}$ (130 g) was stirred in 0.5 M HCl solution for 1.5 h at ambient temperature. After stirring, the product hydrated titanate (HTO) was collected by filtration and washed with water. The HTO was ion-exchanged, 72% of potassium ion and 99% or more lithium ion to protons. The chemical composition was determined by X-ray fluorescence analysis.

The recovered HTO and *N*-(cocoalkyl)-*N,N*-(bis(2-hydroxyethyl))-*N*-methylammonium chloride (157.5 g) were stirred at 80°C for 1 h in double-distilled water. After 1 h, the product was filtered and washed at 80°C with water. The organo-HTO was first dried at 40°C for 1 day under air to prevent particle aggregation, and then at 160°C for 12 h under vacuum.

For nanocomposite preparation, the organo-HTO (OHTO) (dried at 120°C for 8 h) and PLA were first dry-mixed by shaking them in a bag. The mixture was then melt-extruded using a twin-screw extruder (KZW15-30TGN, Technovel Corp., Japan) operated at 195°C (screw speed 300 rpm, feed rate 22 g/min) to yield nanocomposite strands. XRD patterns and TEM observations show the formation of intercalated structured.

Nishida et al. (2005) reported the preparation of aluminum hydroxide ($Al[OH]_3$)-based nanocomposites of PLA to achieve the chemical recycling of flame-resistant properties of PLA. For the preparation of PLLA/$Al(OH)_3$ hybrids, PLLA was first synthesized by the ring-opening polymerization of L,L-lactide catalyzed by Sn(2-ethylhexanoate)$_2$. The polymerized PLLA was purified in a three-stage process: first extracting the catalyst and residues from the PLLA/chloroform solution with a 1 M HCl aqueous solution, then washing with distilled water until the aqueous phase became totally neutral, and finally precipitating the polymer with methanol before vacuum drying. The purified PLLA was then mixed with $Al(OH)_3$ in a prescribed weight ratio in a chloroform solution and vigorously stirred for 1 h to disperse the inorganic particles uniformly. The mixture was then cast on glass Petri dishes.

16.5 PROPERTIES OF PLA NANOCOMPOSITES

Nanocomposites consisting of PLA and nano-fillers frequently exhibit significant improvement in mechanical and various other properties compared with those of pure polymers. Improvements generally include a higher modulus both in solid and the melt states, increased strength and thermal stability, decreased gas permeability, and increased rate of degradability.

Dynamic mechanical analysis (DMA) has been used to study the temperature dependence of G' of PLA upon nanocomposite formation under different experimental conditions. Figure 16-2 shows the temperature dependence of G' for various PLA/clay nanocomposites and pristine PLA. For all PLACNs, the enhancement of G' can be seen in the investigated temperature range when compared with the neat PLA, indicating that organically modified clay particles have a strong effect on the elastic properties of virgin PLA. Below T_g, the enhancement of G' is clear for all nanocomposites. On the other hand, all PLACNs show a greater increase in G' at high temperature compared to that of the PLA matrix. This is due to both mechanical

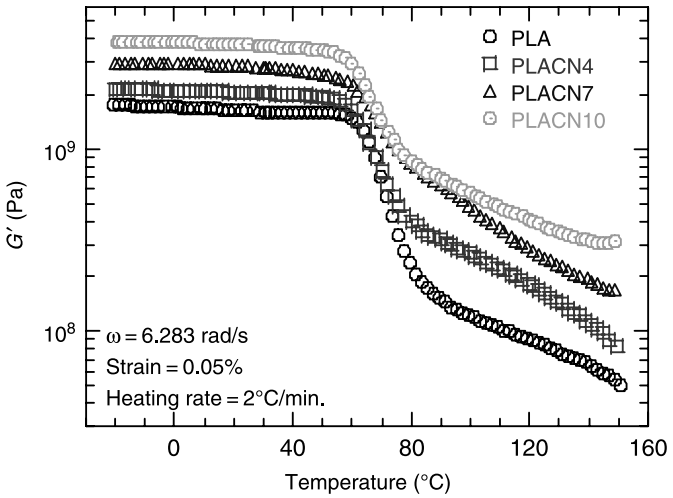

Fig. 16-2 Temperature dependence of storage modulus (G') of neat PLA and various PLACNs prepared with organically modified synthetic fluorine mica. The number indicates amount of organoclay loading.

reinforcement by the silicate layers and extended intercalation at high temperature (Sinha Ray and Okamoto, 2003b). Above T_g, when materials become soft, the reinforcement effect of the silicate layers becomes prominent due to the restricted movement of the polymer chains. This is accompanied by the observed enhancement of G'.

The tensile modulus of polymeric materials has been shown to be remarkably improved when nanocomposites are formed with various types of nano-fillers. In the case of PLA-based nanostructured materials, most studies report the tensile properties as a function of filler content. In most conventionally filled polymer systems, the modulus increases linearly with the filler volume fraction, whereas for these nanoparticles at much lower filler concentrations, the modulus increased sharply and to a much larger extent. The dramatic enhancement of the modulus for such extremely low clay concentrations cannot be attributed simply to the introduction of the higher modulus inorganic filler layers.

A theoretical approach assumes a layer of affected polymer on the filler surface, with a much higher modulus than the bulk equivalent polymer (Shia et al., 1998). This affected polymer can be thought of as the region of the polymer matrix that is physisorbed onto the silicate surface and is thus stiffened through its affinity for and adhesion to the filler surfaces (Shia et al., 1998). For such high-aspect-ratio fillers as our layered silicate layers, the surface area exposed to the polymer is huge and the significant increases in the modulus with very low filler content are not surprising. Furthermore, beyond the percolation limit the additional silicate layers are incorporated into polymer regions that are already affected by other silicate layers, and thus it is expected that the enhancement of modulus will be much less dramatic.

Lee et al. (2003) reported the MMT content dependence of tensile modulus of PLLA nanocomposites scaffolds. The modulus of the nanocomposites systematically increased with increasing MMT loading. According to these authors, the crystallinity and the glass transition temperature of PLLA nanocomposites were lower than those of neat PLLA, but the modulus of neat PLLA was significantly increased in the presence of a small amount of MMT loading. This observation suggests that the layered silicates of MMT act a mechanical reinforcement of polymer chains.

In the case of PLLA/MWCNT nanocomposites, it was observed that the Young's modulus increases with MWCNT loading in the nanocomposite films compare to pure PLLA films, although an increase in the MWCNT content did not cause a significant increase in Young's modulus. The average Young's modulus of the 5 wt% nanocomposite was approximately 2.5 GPa, which was approximately 150% higher than that of the pure PLLA film. It was also observed that increasing the loading of MWCNTs in these nanocomposites caused a significant increase in stiffness, which eventually led to brittle fracture, as indicated by the low elongation at break in the tensile test.

Sinha Ray and co-workers reported the detailed measurement of flexural properties of neat PLA and various nanocomposites prepared with organoclay (Sinha Ray et al., 2003a). They conducted flexural property measurements with injection-molded samples according to the ASTM D-790 method. There was a significant increase in flexural modulus for nanocomposite prepared with 4 wt% of organoclay when compared to that of neat PLA, followed by a much slower increase with increasing organoclay content, and a maximum of 50% for nanocomposite prepared with 10 wt% of organoclay. On the other hand, the flexural strength showed a remarkable increase with PLACN7 (nanocomposite prepared with 7 wt% clay), and then gradually decreased with organoclay loading. According to the authors, this behavior may be due to the high clay content, which leads to brittleness in the material. They also measured the flexural properties of PLA nanocomposites prepared with various kinds of organically modified MMT, and the results showed a similar trend. This means that there is an optimal amount of organoclay needed in a nanocomposite to achieve the greatest improvement in its properties.

Generally, the incorporation of nano-fillers into the polymer matrices was found to enhance the thermal stability by acting as a superior insulator and mass transport barrier to the volatile products generated during decomposition. Bandyopadhyay et al. (1999) reported the first improved thermal stability of nanostructured materials that combined PLA and organically modified fluorohectorite (FH) or MMT clay. These nanocomposites were prepared by melt intercalation. The authors showed that the PLA that was intercalated between the galleries of FH or MMT clay resisted the thermal degradation under conditions that would otherwise completely degrade pure PLA. They argue that the silicate layers act as a barrier for both the incoming gas and also the gaseous by-products, which increases the degradation onset temperature and also widens the degradation process. The addition of clay enhances the performance of the char formed, by acting as a superior insulator and mass transport barrier to the volatile products generated during decomposition. Recently, there have been many reports concerned with the improved thermal stability of PLA-based

nanocomposites prepared with various kinds of organically modified layered silicates (OMLS) (Paul et al., 2003). Chang et al. (2003b) conducted detailed thermogravimetric analyses of PLA-based nanocomposites of three different OMLS. In the case of C16MMT- or C25A-based hybrids, the initial degradation temperatures (T_{iD}) of the nanocomposites decreased linearly with increasing amount of OMLS. On the other hand, in nanocomposite prepared with DTAMMT clay, the initial degradation temperature was nearly constant over code of clay loadings from 2 to 8 wt%. This observation indicates that the thermal stability of the nanocomposites is directly related to the stability of OMLS used for the preparation of nanocomposites.

Paul et al. (2003) prepared PLA layered silicate nanocomposites by melt intercalation in the presence of a stabilizer to decrease the possibility of host matrix degradation due to heating. The degradation of PLA during processing takes place even in the presence of antioxidant, and 41.2% decrease in number average molecular weight was observed compared with native PLA. An increase in the thermal stability under oxidative conditions was found and it was suggested that a physical barrier between the polymer medium and superficial zone of flame combustion may be generated due to the char formation. The use of PLA for automotive parts has been studied as a possible contribution to restraining the increase in CO_2 emissions. For this application, major improvements in heat and impact resistance are needed. It was found that in-mold crystallization of the PLA/clay nanocomposite led to a large suppression of the decrease in storage modulus at high temperature, which in turn improved the heat resistance of PLA.

16.6 BIODEGRADABILITY

The degradation process of aliphatic polyesters is a complex process, which can proceed via hydrolysis (most often catalyzed by enzymes) and/or oxidation (UV- or thermo-induced). The stereoconfiguration and possible crystallinity, relative hydrophobicity of the polymer matrix, presence of substituents, or even filler and conformational flexibility contribute to the biodegradability of synthetic polymers with hydrolysable and/or oxidizable linkages in their main chain. On the other hand, the morphology of the polymer samples or the material structure as recovered after loading with given filler; greatly affect their rate of biodegradation.

A major problem with the PLA matrix is the very slow rate of degradation. Despite the considerable number of reports concerning the enzymatic degradation of PLA (Gruber and Brien, 2002) and various PLA blends (Sinha Ray and Bousmina, 2005) very little is reported about the composting degradability of PLA, except in recent publications by the Sinha Ray and co-workers (Sinha Ray et al., 2003d; Sinha Ray and Bousmina, 2005). Figure 16-3 illustrates samples recovered from compost after various times.

Sinha Ray and his group also conducted a respirometric test to study the degradation of the PLA matrix in a compost environment (Sinha Ray et al., 2002c, 2003d). For this test the compost used was prepared from a mixture of bean-curd refuse, food waste, and cattle feces. Unlike weight loss or fragmentation, which

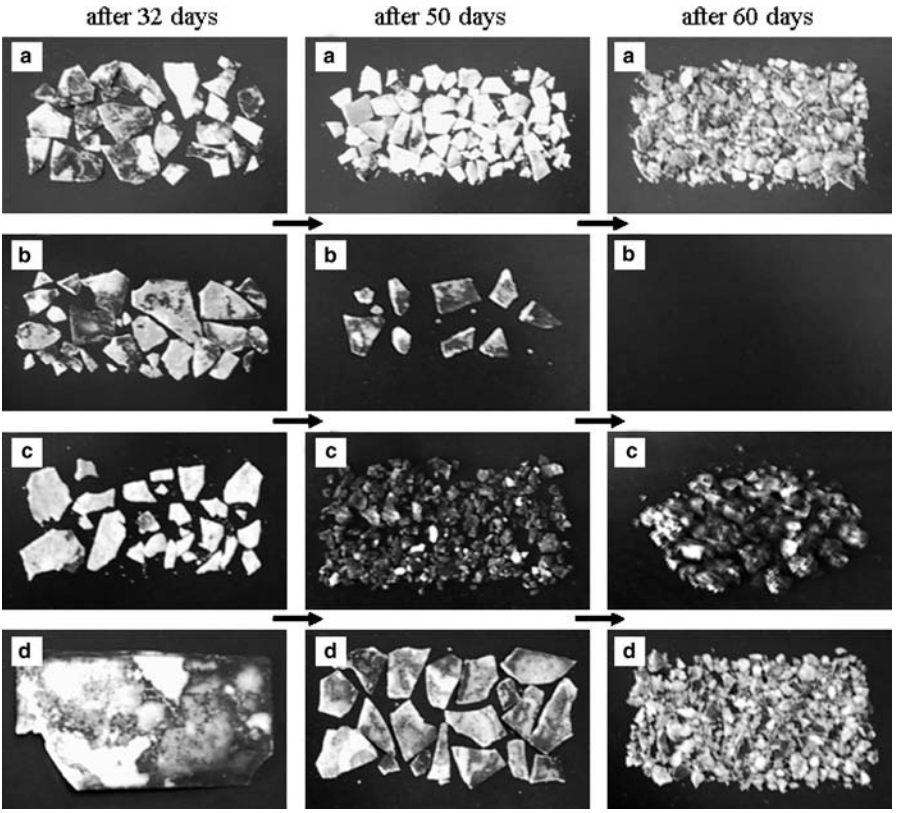

Fig. 16-3 Biodegradability of (a) neat PLA, (b) PLA/qC18-MMT4, (c) PLA/C18-MMT4, and (d) PLA/qC18-Mica4 recovered from compost after various times. The initial shape of the crystallized samples was 3 cm × 10 cm × 0.1 cm.

reflects the structural changes in the test sample, CO_2 evolution provides an indicator of the ultimate biodegradability, that is, mineralization, of the test samples. Experimental results clearly indicate that the biodegradability of the PLA component in PLA/qC13(OH)-mica4 or PLA/qC16-SAP4 was enhanced significantly. On the other hand, the PLA component in PLA/C18-MMT4 shows a slightly higher biodegradation rate, while the rates of degradation of pure PLA and PLA/qC18-MMT4 are almost the same. The compost degradation of PLA occurs by a two-step process. During the initial phases of degradation, the high-molecular-weight PLA chains hydrolyze to lower-molecular-weight oligomers. This reaction can be accelerated by acids or bases and is also affected by both temperature and moisture. Fragmentation of the plastic occurs during this step at a point where the M_n decreases to less than about 40,000. At about this same M_n value, microorganisms in the compost environment continue the degradation process by converting these lower-molecular-weight components to CO_2, water, and humus (Ikada and Tsuji, 2000; Gruber and Brien, 2002). Therefore, any factor that increases the tendency to hydrolysis of the PLA matrix ultimately controls the degradation of PLA.

The incorporation of OMLS fillers into the PLA matrix resulted in a small reduction in the molecular weight of the matrix. It is well known that PLA of relatively low molecular weight may show higher rates of enzymatic degradation because of, for example, the high concentration of accessible chain end groups (Sinha Ray et al., 2003d). However, in these cases the rate of molecular weight change of pure PLA and PLA in various nanocomposites is almost the same. Thus the initial molecular weight is not the main factor controlling the degradability of nanocomposites. Another factor that controls degradability of PLA in nanocomposite is the different degree of dispersion of silicate layers in the polymer matrix, which actually depends on the nature of the surfactant used to modify the clay surface. Therefore, we can control the degradability of PLA by judicious choice of OMLS.

To understand to what extent the incorporation of pristine and organically modified clay influences the degradation behavior of the PLA matrix, Paul et al. (2003) conducted the hydrolytic degradation of composites based on the same amounts (3 wt%) of Cloisite Na^+, Cloisite 25A, and Cloisite 30B for more than 5 months, directly compared with the pure PLA. In a typical experimental procedure, the samples were first shaped as films about 0.5 mm thick. In a second step, each film was cut into 1.3 cm $\times$ 3.0 cm rectangular specimens (three specimens per sample). Each specimen was then dipped in a flask containing 25 ml of 0.1 M phosphate buffer at pH 7.4. The flasks were immersed in a water bath at 37°C. At predetermined periods (1 week, 2 weeks, 1 month, 2.5 months, and 5.5 months) the specimen were picked out of the buffered solution and rinsed several times with distilled water. Finally, the residual water was wiped off from the sample surface before drying it by wrapping it in a small paper bag placed in a desiccator.

The results indicated that faster hydrolysis, leading to an increase of the crystallinity of the PLA matrix, is found for the Cloisite Na^+-based blend, that is, that it is due to the microcomposite structure. It was also concluded that both composite structure, either microcomposite or intercalated nanocomposite, and the relative hydrophilicity of the clay play determining roles in the hydrolytic degradation process. Indeed, the more hydrophilic the filler, the more pronounced is the degradation.

16.7 MELT RHEOLOGY

In the case of polymer nanocomposites, measurements of melt rheological properties are not only important for understand the processability of these materials but are also helpful in elucidating the strength of the polymer–filler and the structure–property relationships in nanocomposites. This is because rheological behavior is strongly influenced by nanoscale structure and interfacial characteristics.

From the master curves for G' and G'' of pure PLA and various nanocomposites with different weight percentages of C18MMT loading, at high frequencies ($a_T\omega > 10$ rad/s), the viscoelastic behavior was the same for all nanocomposites. In contrast, at low frequencies ($a_T\omega < 10$ rad/s), both moduli exhibited weak frequency dependence with increasing C18MMT content, such that there are gradual

changes of behavior from liquidlike (G' and $G'' \propto \omega$) to solidlike with increasing C18MMT content (Sinha Ray and Okamoto, 2003b).

The slopes of G' and G'' in the terminal region of the master curves of the PLA matrix were 1.85 and 1, respectively, values in the range expected for polydisperse polymers (Hoffmann et al., 2000). On the other hand, the slopes of G' and G'' were considerably lower for all PLACNs compared to those of pure PLA. In fact, for PLACNs with high C18MMT content, G' becomes nearly independent at low $a_T\omega$ and exceeds G'', characteristic of materials exhibiting a pseudo solidlike behavior.

In the dynamic complex viscosity $|\eta^*|$ master curves for the pure PLA and nanocomposites, based on linear dynamic oscillatory shear measurements, in the low $a_T\omega$ region (<10 rad/s), pure PLA exhibited almost newtonian behavior while all nanocomposites showed very strong shear-thinning tendency. On the other hand, M_w and PDI (Poly dispersity index) of pure PLA and various nanocomposites were almost the same; thus the high viscosity of PLACNs was explained by the flow restrictions of polymer chains in the molten state due to the presence of MMT particles.

The shear rate-dependent viscosity of pure PLA and various PLACNs at 175°C was also measured by Sinha Ray and Okamoto (2003b). The pure PLA exhibited almost newtonian behavior at all shear rates, whereas PLACNs exhibited nonnewtonian behavior. All PLACNs showed a very strong shear-thinning behavior at all measured shear rates and this behavior is analogous to the results obtained in the case of oscillatory shear measurements. Additionally, at very high shear rates, the steady shear viscosities of PLACNs were comparable to that of pure PLA. These observations suggest that the silicate layers are strongly oriented toward the flow direction (perhaps perpendicular alignment of the silicate layers toward the stretching direction) at high shear rates, whereas pure polymer dominates shear-thinning behavior at high shear rates.

Sinha Ray and Okamoto (2003b) first conducted elongation tests of PLA/clay nanocomposite prepared with 5 wt% of C18MMT in the molten state at constant Hencky strain rate, $\dot{\varepsilon}_0$ using elongation rheometry. On each run of the elongation test, samples of size 60 mm × 7 mm × 1 mm^3 were annealed at a predetermined temperature for 3 min before starting the run in the rheometer, and uniaxial elongation experiments were conducted at various $\dot{\varepsilon}_0$ values. Figure 16-4 shows double-logarithmic plots of the transient elongation viscosity $\eta_E(\dot{\varepsilon}_0; t)$ versus time t, observed for PLACN5 (nanocomposite prepared with 5 wt% of clay) at 170°C with various $\dot{\varepsilon}_0$ values ranging from 0.01 to 1.0 s^{-1}. The figure shows a strong *strain-induced hardening* behavior for PLACN5. In the early stage, η_E gradually increases with t but is almost independent of $\dot{\varepsilon}_0$. This is generally called the *linear region* of the viscosity curve. After a certain time, t_{η_E}, which is the *up-rising* time (marked with the upward arrows in the figure), η_E was strongly dependent on $\dot{\varepsilon}_0$, and a rapid upward deviation of η_E from the curves of the linear region was observed. The authors tried to measure the elongational viscosity of pure PLA but they were unable to do so accurately; the low viscosity of pure PLA may be the main reason. However, they confirmed that neither strain-induced hardening in elongation nor rheopexy in shear flow took place in the case of pure PLA having the same molecular weight and polydispersity as PLACN3.

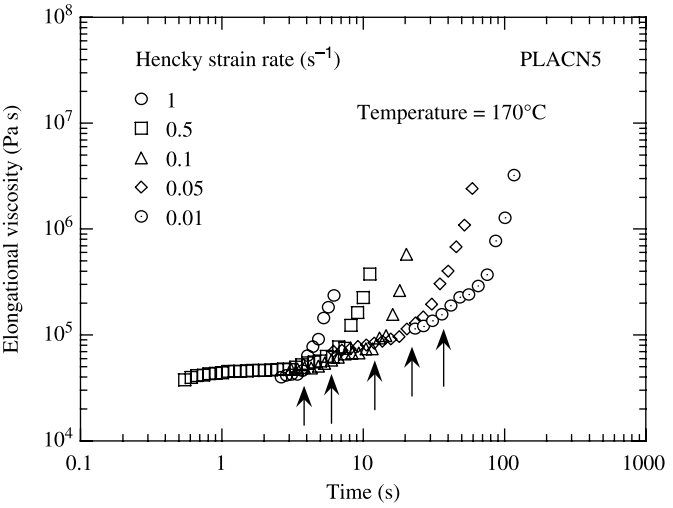

Fig. 16-4 Strain rate dependence of up-rising Hencky strain. Reproduced from Sinha Ray and Okamoto (2003b) by permission of Wiley-VCH Verlag GmbH, Germany.

As in polypropylene/OMLS systems, the extended Trouton rule, $3\eta_0(\dot{\gamma};t) \cong \eta_E(\dot{\varepsilon}_0;t)$, does not hold for PLACN5 melt, as opposed to the melts of pure polymers (Okamoto et al., 2001a; Nam et al., 2002). These results indicate that in the case of PLACN5, flow-induced internal structural changes also occurred in elongation flow, but the changes were quite different from those in shear flow. The strong rheopexy observed in shear measurements for PLACN5 at very slow shear rates reflected the fact that the shear-induced structural change involved a process with an extremely long relaxation time.

16.8 FOAM PROCESSING

Polymeric foams have become widely used as packing materials because they are lightweight, have a high strength/weight ratio, have superior insulating properties, and have high energy-absorbing performance. One of the most widely used polymers for the preparation of foam is PS (polystyrene). It is produced from fossil fuels, consumed, and discarded into the environment, ending up as waste that is not spontaneously degradable. Use of foams made from biodegradable polymeric materials would alleviate this problem.

Biodegradable polymers such as PLA have some limitations in foam processing because such polymers do not exhibit high strain-induced hardening, which is the primary requirement to withstand the stretching forces experienced during the latter stages of bubble growth. Branching of polymer chains, grafting with another copolymer, or blending of branched and linear polymers are the common methods used to improve the extensional viscosity of a polymer in order to make it suitable for foam

formation. PLACNs have already been shown to exhibit a high modulus and, under uniaxial elongation, a tendency toward strong strain-induced hardening. On the basis of these results, Sinha Ray and his group (Sinha Ray and Okamoto, 2003b) first conducted foam processing of PLACNs with the expectation that they would provide advanced polymeric foams with many desirable properties. They used a physical foaming method, a batch process, for foam processing. This process consists of four stages: (a) saturation of CO_2 in the sample at the desired temperature; (b) cell nucleation when the release of CO_2 pressure begins (forming supersaturated CO_2); (c) cell growth to an equilibrium size during the release of CO_2; and (4) stabilization of the cell via cooling of the foamed sample.

Figure 16-5 shows typical SEM images of the freeze-fracture surfaces of neat PLA and two different nanocomposites foamed at 140°C for PLA and PLA/C18MMT5 and at 165°C for PLA/qC18MMT5. All foams exhibited a nice closed-cell structure with homogeneous cells in the case of nanocomposites, while the neat PLA foam showed nonuniform cell structure having large cell size (~230 μm). Also, the nanocomposite foams showed a smaller cell size (d) and larger cell density (N_c) than neat PLA foam, suggesting that the dispersed silicate particles act as nucleating sites for cell formation (Okamoto et al., 2001b). They calculated the distribution function of cell size from SEM images and showed that the nanocomposite foams nicely

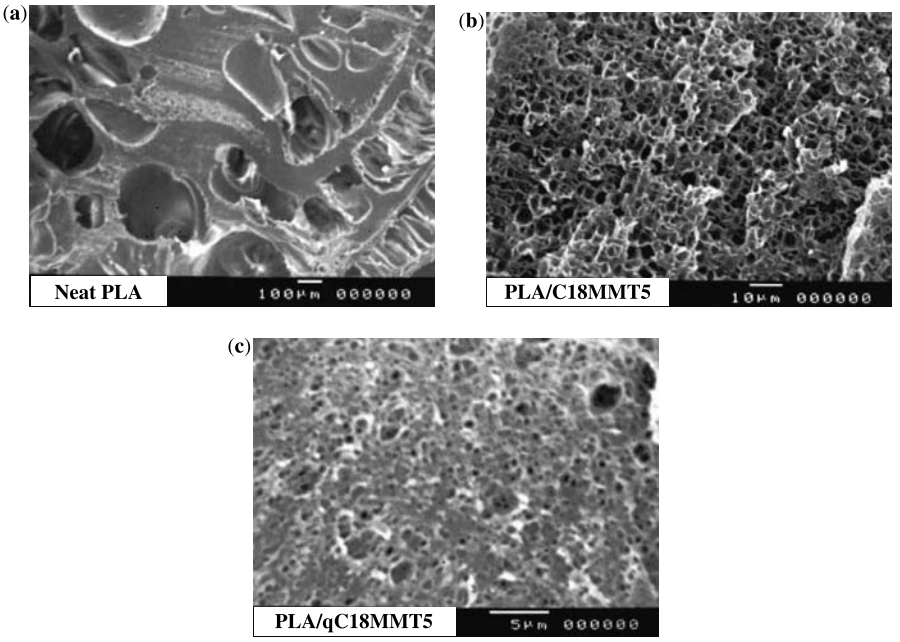

Fig. 16-5 SEM images of freeze-fracture surfaces of (a) neat PLA, (b) PLA/C18MMT5, and (c) PLA/qC18MMT5 foams. Reproduced from Fujimoto, Sinha Ray, Okamoto, Ogami and Ueda by permission of Wiley-VCH Verlag GmbH, Germany.

obeyed a Gaussian distribution. In the case of PLA/qC18MMT5 (Fig. 16-5b), the width of the distribution peaks, which indicates the dispersity for cell size, became narrow and were accompanied by a finer dispersion of silicate particles. The PLA/qC18MMT5 (nanocellular) foam has a smaller d value ($\sim$360 nm) and a huge N_c (1.2×10^{14} cells/cm^{-3}) compared with PLA/C18MMT5 (microcellular) foam ($d = 2.59\,\mu$m and $N_c = 3.56 \times 10^{11}$ cells/cm^{-3}) (Sinha Ray and Okamoto, 2003b). These results indicate that the nature of the dispersion plays a vital role in controlling the size of the cell during foaming. On the other hand, the very high value of N_c for the PLA/qC18MMT5 foam indicates that the final ρ_f value is controlled by the competitive processes in cell nucleation, growth, and coalescence. The cell nucleation, in the case of the nanocomposite systems, took place in the boundary between the matrix polymer and the dispersed silicate particles. For this reason, the cell growth and coalescence were strongly affected by the characteristic parameter and the storage and loss modulus ($\approx$ viscosity component) of the materials during processing. This may create nanocellular foams without the loss of mechanical properties in the case of polymeric nanocomposites.

16.9 POTENTIAL FOR APPLICATIONS AND FUTURE PROSPECTS

New environmental polices, societal concerns, and growing environmental awareness have triggered the search for new products and processes that are benign to the environment. PLA is considered as an alternative to the existing petroleum-based plastic materials, but the intrinsic properties of unmodified PLA, such as its high crystallinity ($\sim$40%) and rigidity and slow degradation, put limits on its wide applicability (Leaversuch, 2002; Gupta, 2007). PLA-based nanostructured materials offer unique combinations of properties, including biodegradability and thermoplastic processibility, that offer potential applications as commodity plastics, such as in packaging, agricultural products, and disposable materials. The versatility of the nano-fillers used with respect to transformation into various shapes and morphologies along with good mechanical properties offers a wide range of applications.

The thermoplastic character of PLA is very useful in allowing transformation of the polymer materials into various shapes. The apparel sector is very promising. For example, the University of Tennessee (USA) has been active in work on spunlaid and melt-blown nonwovens based on PLA. Kanebo Ltd (Japan) has produced a PLA fiber under the brand name LACTRON^{TM}, which was exhibited in garments during the Nagano Olympics under the umbrella of "Fashion for the Earth" (Lunt and Shafer, 2000). The low modulus of the fiber has been exploited for better drape and feel of fabrics. A market for PLA and PLA-based nanostructured materials has also developed in sportswear, especially as an inner wicking layer.

Polylactide-based nanocomposites are an important part of the family of novel biomaterials though their history is no more than 10 years. From the considerations of versatile properties and wide range of possible applications, these materials have attracted a great deal of scientific and industrial interest and have led research in

biomaterials science in new directions. This chapter has provided a snapshot of the synthesis and characterization procedures for PLA and various PLA-based nanostructured materials. Useful progress has been made to date toward improvement of the processability and potential for application of pure PLA to make it suitable for wide range of applications from commodity plastics to medical applications. By changing the nature of the nano-fillers and the processing conditions, some of the physical properties of pure PLA—mechanical, thermal, and electrical properties, biodegradability, etc.—have been improved significantly, which was not possible by simple mixing with conventional fillers. Considering the progress to date of research in this field, it can be concluded that these materials will be commercially available very soon and their appropriate utilization will open further research directions.

REFERENCES

Alexander M, Doubis P. 2000. Polymer-layered silicate nanocomposites, properties and uses of a new class of materials. *Mater Sci Eng* R28:1.

Andrews R, Weisenberger MC. 2004. Carbon nanotube polymer composites. *Curr Opin Solid State Mater Sci* 8:31.

Awasthi K, Srivastava A, Srivastava ON. 2005. Synthesis of carbon nanotubes. *J Nanosci Nanotechnol* 5:1616.

Baibarac M, Gomez-Romero P. 2006 Nanocomposites based on conducting polymers and carbon nanotubes: From fancy materials to functional applications. *J Nanosci Nanotechnol* 6:289–302.

Bandyopadhyay S, Chen R, Giannelis EP. 1999. Polylactic acid layered silicate nanocomposites. *Polym Mater Sci Eng* 81:159.

Banerjee S, Hemraj-Benny T, Wong SS. 2005. Routes towards separating metallic and semiconducting nanotubes. *J Nanosci Nanotechnol* 5:841.

Bischoff CA, Walden P. 1894. Synthesis of polyglycolic and polyglycolic acid. *Liebigs Ann Chem* 279:45–51.

Biswas M, Sinha Ray S. 2001. Recent progress in synthesis and evaluation of polymer-montmorillonite nanocomposites. *Adv Polym Sci* 155:167.

Brindly SW, Brown G. 1980. *Crystal Structure of Clay Minerals and their X-ray Diffraction*. London: The Mineralogical Society.

Chang JH, An YU, Sur GS. 2003a. Poly(lactic acid) nanocomposites with various organoclays. I. Thermomechanical properties, morphology, and gas permeability. *J Polym Sci Part B: Polym Phys* 41:94.

Chang JH, An YU, Cho D, Giannelis EP. 2003b. Poly(lactic acid) nanocomposites: comparison of their properties with montmorillonite and synthetic mica (II). *Polymer* 44:3715.

Chen GX, Kim HS, Park BH, Yoon JS. 2005. Controlled functionalization of multiwalled carbon nanotubes with various molecular-weight poly(L-lactic acid). *J Phys Chem B* 109:22237.

Cui X, Engelhard MH, Lin Y. 2006. Preparation, characterization and anion exchange properties of polypyrrole/carbon nanotube nanocomposites. *J Nanosci Nanotechnol* 6:547–553.

Drumright RE, Gruber PR. 2000. Polylactic acid technology. *Adv Mater* 23:1841.

Enomoto K, Ajioka M, Yamaguchi A. 1994. Polyhydroxycarboxylic acid and preparation process thereof. US Patent 5,310,865.

Fang Q, Hanna MA. 1999. Rheological properties of amorphous and semicrystalline polylactic acid polymers. *Ind Crops Prod* 10:47.

Fernando KAS, Lin Y, Zhou B, et al. 2005. Poly(ethylene-*co*-vinyl alcohol) functionalized single-walled carbon nanotubes and related nanocomposites. *J Nanosci Nanotechnol* 5:1050.

Fujimoto Y, Sinha Ray S, Okamoto M, Ogami A, Yamada K, Ueda K. 2003. Well-controlled biodegradable nanocomposite foams: from microcellular to nanocellular. *Macromol Rapid Commun* 24:457–461.

Gruber P, Brien MO. 2002. Polylactides NatureWorks™ PLA. In: Doi Y, Steinbuchel A, editors. *Biopolymers*, Volume 4, Polyesters III Applications and Commercial Products. Weinheim: Wiley-VCH. p. 235.

Gu JD, Gada M, Kharas G, Eberiel D, McCarthy SP, Gross RA. 1992. *Polym Mater Sci Eng* 67:351.

Gupta B, Revagade N, Hilborn J. 2007. Poly(lactic acid) fiber: an overview. *Prog Polym Sci* 32:455.

Hiroi R, Sinha Ray S, Okamoto M, Shiroi T. 2004. Organically modified layered titanate: a new nanofiller to improve the performance of biodegradable polylactide. *Macromol Rapid Commun* 25, 1359.

Hoffmann B, Kressler J, Stoppelmann G, Friedrich Chr, Kim GM. 2000. Rheology of nanocomposites based on layered silicates and polyamide-12. *Colloid Polym Sci* 278:629.

Ikada Y, Tsuji H. 2000. Biodegradable polyesters for medical and ecological applications. *Macromol Rapid Commun* 21:117.

Kim HW, Lee HH, Knowles CJ. 2006. Electrospinning biomedical nanocomposite fibers of hydroxyapatite/poly(lactic acid) for bone regeneration. *J Biomed Mater Res* 79A:643.

Kim K, Cho SJ, Kim ST, Chin IJ, Choi HJ. 2005. Formation of two-dimensional array of multiwalled carbon nanotubes in polystyrene/poly(methyl methacrylate) thin film. *Macromolecules* 38:10623.

Kramschuster A, Gong S, Turng LS, Li T. 2007. Injection-molded solid and microcellular polylactide and polylactide nanocomposites. *J Biobased Mater Bioenergy* 1:37.

Krikorian V, Pochan DJ. 2003. Poly (L-lactic acid)/layered silicate nanocomposite: fabrication, characterization, and properties. *Chem Mater* 15:4317.

LeBaron PC, Wang Z, Pinnavaia TJ. 1999. Polymer-layered silicate nanocomposites: an overview. *Appl Clay Sci* 15:11–35.

Lee JH, Park TG, Park HS, et al. 2003. Thermal and mechanical characteristics of poly(L-lactic acid) nanocomposite scaffold. *Biomaterials* 24:2773.

Leaversuch R. 2002. Renewable PLA polymer gets 'green light' for packaging uses. *Plastic Technology*. On-line article: www.plastictechnology.com/articles/200209fa3.html.

Lipinsky ES, Sinclair RG. 1986. Is lactic acid is a commodity chemical? *Chem Eng Prog* 82:26–32.

Lunt J. 1998. Large-scale production, properties and commercial applications of polylactic acid polymers. *Polym Degrad Stab* 59:149.

Lunt J, Shafer AL. 2000. Polylactic acid polymers from corn, Applications in the textiles industry. *J Ind Text* 29:191.

Maiti P, Yamada K, Okamoto M, Ueda K, Okamoto K. 2002. New polylactide/layered silicate nanocomposites: role of organoclays. *Chem Mater* 14:4654.

Mark JE. 2006. Some novel polymeric nanocomposites. *Acc Chem Res* 39, 881.

Martin O, Averous L. 2001. Poly(lactic acid): plasticization and properties of biodegradable multiphase systems. *Polymer* 42:6209.

Miyagawa H, Misra M, Mohanty AK. 2005. Mechanical properties of carbon nanotubes and their polymer nanocomposites. *J Nanosci Nanotechnol* 5:1593–1615.

Mohanty AK, Drzal LT, Misra M. 2003. Nano reinforcements of bio-based polymers—the hope and the reality. *Polym Mater Sci Eng* 88:60.

Moon S, Jin F, Lee CJ, Tsutsumi S, Hyon SH. 2005. Novel carbon nanotube/poly(L-lactic acid) nanocomposites; their modulus, thermal stability, and electrical conductivity. *Macromol Symp* 224:287.

Nam PH, Maiti P, Okamoto M, et al. 2002. Foam processing and cellular structure of polypropylene/clay nanocomposites. *Polym Eng Sci* 42:1907.

Nam PH, Fujimori A, Masuko T. 2004a. Flocculation characteristics of organo-modified clay particles in poly(L-lactide)/montmorillonite hybrid systems. *e-Polymers* 005. http://www.e-polymers.org/.

Nam PH, Fujimori A, Masuko T. 2004b. The dispersion behavior of clay particles in poly(L-lactide)/organo-modified montmorillonite hybrid systems. *J Appl Polym Sci* 93:2711.

Nam PH, Kaneko M, Ninomiya N, Fujimori A, Masuko T. 2004c. Melt intercalation of poly(L-lactide) chains into clay galleries. *Polymer* 46:7403.

Nazhat SN, Kellomaki M, Tormala P, Tanner KE, Bonfield W. 2001. Dynamic mechanical characterization of biodegradable composites of hydroxyapatite and polylactides. *J Biomed Mater Res* 58:335.

Ninomiya N, Nam PH, Fujimori A, Masuko T. 2004. Distribution of clay particles in the spherulitic texture of poly(L-lactide)/organo-modified montmorillonite hybrids. *e-Polymers* 41. http://www.e-polymers.org/.

Nishida H, Fan Y, Mori T, Oyagi N, Shirai Y, Endo T. 2005. Feedstock recycling of flame-resisting poly(lactic acid)/aluminum hydroxide composite to L,L-lactide. *Ind Eng Chem Res* 44:1433.

Ogata N, Jimenez G, Kawai H, Ogihara T. 1997. Structure and thermal/mechanical properties of poly(L-lactide)-clay blend. *J Polym Sci Part B: Polym Phys* 35:389.

Okamoto M, Nam PH, Maiti M, et al. 2001a. Biaxial flow-induced alignment of silicate layers in polypropylene/clay nanocomposite foam. *Nano Lett* 1:503.

Okamoto M, Nam PH, Maiti P, Kotaka T, Hasegawa N, Usuki A. 2001b. A house of cards structure in polypropylene/clay nanocomposites under elongational flow. *Nano Lett* 1:295.

Paul MA, Alexandre M, Degee P, Henrist C, Rulmont A, Dubois P. 2003. New nanocomposite materials based on plasticized poly(L-lactide) and organo-modified montmorillonites: thermal and morphological study. *Polymer* 44:443.

Paul MA, Delcourt C, Alexandre M, Degee Ph, Monteverde F, Dubois Ph. 2005. Polylactide/montmorillonite nanocomposites: study of the hydrolytic degradation. *Polym Degrad Stab* 87:535.

Pelouze J. 1845. Synthesis of low-molecular weight polylactic acid. *Ann Chimie* 13:257–262.

Shi X, Hudson JL, Spicer PP, Tour JM, Krishnamoorti R, Mikos AG. 2006. Injectable nanocomposites of single-walled carbon nanotubes and biodegradable polymers for bone tissue engineering. *Biomacromolecules* 7:2237.

Shi X, Hudson JL, Spicer PP, Tour JM, Krishnamoorti R, Mikos AG. 2005. Rheological behaviour and mechanical characterization of injectable poly(propylene fumarate)/single-walled carbon nanotube composites for bone tissue engineering. *Nanotechnology* 16:S531.

Shia D, Hui CY, Burnside SD, Giannelis EP. 1998. An interface model for the prediction of Young's modulus of layered silicate-elastomer nanocomposites. *Polym Compos* 19:608.

Sinha Ray S. 2006. Rheology of polymer/layered silicate nanocomposites. *J Ind Eng Chem* 12:811.

Sinha Ray S. 2007. In: Nalwa HS, editor. Clay containing polymer nanocomposites. *Polymeric Nanostructures and Their Applications*, Volume 1, Chapter 1. Los Angeles: American Scientific Publishers.

Sinha Ray S, Bousmina M. 2005. Biodegradable polymer and their layered silicate nanocomposite: In greening the 21st century materials science. *Prog Mater Sci* 50:962–1079.

Sinha Ray S, Okamoto M. 2003a. Polymer/layered silicate nanocomposites: a review from preparation to processing. *Prog Polym Sci* 28:1539.

Sinha Ray S, Okamoto M. 2003b. Polylactide/layered silicate nanocomposites.6. Melt rheology and foam processing. *Macromol Mater Eng* 288:936.

Sinha Ray S, Yamada K, Ogami A, Okamoto M, Ueda K. 2002a. New polylactide/layered silicate nanocomposite: Nanoscale control over multiple properties. *Macromol Rapid Commun* 23:493.

Sinha Ray S, Maiti P, Okamoto M, Yamada K, Ueda K. 2002b. Polylactide/layered silicate nanocomposites. 1. Preparation, characterization and properties. *Macromolecules* 35:3104.

Sinha Ray S, Yamada K, Okamoto M, Ueda K. 2002c. Polylactide/layered silicate nanocomposite: A novel biodegradable material. *Nano Lett* 2:1093.

Sinha Ray S, Okamoto K, Okamoto M. 2003a. Structure–property relationship in biodegradable poly(butylene succinate)/layered silicate nanocomposites. *Macromolecules* 36:2355.

Sinha Ray S, Yamada K, Okamoto M, Ogami A, Ueda K. 2003b. Polylactide/layered silicate nanocomposites. Part 3. High performance biodegradable materials. *Chem Mater* 15:1456.

Sinha Ray S, Yamada K, Okamoto M, Fujimoto Y, Ogami A, Ueda K. 2003c. Polylactide/layered silicate nanocomposites. 5. Designing of materials with desired properties. *Polymer* 44:6633–6646.

Sinha Ray S, Yamada K, Okamoto M, Ueda K. 2003d. Polylactide/layered silicate nanocomposite. 2. Concurrent improvements of materials properties, biodegradability and melt rheology. *Polymer* 44:857.

Sinha Ray S, Yamada K, Okamoto M, Ueda K. 2003e. Biodegradable polylactide/montmorillonite nanocomposites. *J Nanosci Nanotechnol* 3:503.

Sinha Ray S, Yamada K, Okamoto M, Ogami A, Ueda K. 2003f. New polylactide/layered silicate nanocomposites, 4. Structure, properties and biodegradability. *Compos Interfaces* 10:435.

Sinha Ray S, Vaudreuil S, Maazouz A, Bousmina M. 2006. Dispersion of multi-walled carbon nanotubes in biodegradable poly(butylene succinate) matrix. *J Nanosci Nanotechnol* 6:2191–2195.

Song W, Zheng Z, Tang W, Wang W. 2007. A facile approach to covalently functionalized carbon nanotubes with biocompatible polymer. *Polymer* 48:3658–3663.

Thostenson ET, Ren ZF, Chou TW. 2001. Advances in the science and technology of carbon nanotubes and their composites: a review. *Compos Sci Technol* 61:1899–1912.

Vaudreuil S, Labzour A, Sinha Ray S, Maazouz A, Bousmina M. 2007. Dispersion characteristics and properties of poly(methyl methacrylate)/multi-walled carbon nanotubes Nanocomposites. *J Nanosci Nanotechnol* 7:2349.

Vink ETH, Rabago KR, Glassner DA, Gruber PR. 2003. Applications of life cycle assessment to NatureWorks™ polylactide (PLA) production. *Polym Degrad Stab* 80:403.

Watson PD. 1948. Lactic acid polymers as constituents of synthetic resins and coatings. *Ind Eng Chem* 40:1393.

Yang Y, Gupta MC, Dudley KL, Lawrence RW. 2005. A comparative study of EMI shielding properties of carbon nanofiber and multi-walled carbon nanotube filled polymer composites. *J Nanosci Nanotechnol* 5:927.

Zanetti M, Lomakin S, Camino G. 2000. Polymer layered silicate nanocomposites. *Macromol Mater Eng* 279:1.

Zhang W, Suhr J, Koratkar N. 2006. Carbon nanotube/polycarbonate composites as multifunctional strain sensors. *J Nanosci Nanotechnol* 6:960.

Zhang XF, Liu T, Sreekumar TV, et al. 2003. Poly(vinyl alcohol)/SWNT composite film. *Nano Lett* 3:1285.

CHAPTER 17

Advances in Natural Rubber/ Montmorillonite Nanocomposites

DEMIN JIA, LAN LIU, XIAOPING WANG, BAOCHUN GUO, and YUANFANG LUO

College of Materials Science and Engineering, South China University of Technology Guangzhou, China

Biodegradable Polymer Blends and Composites from Renewable Resources. Edited by Long Yu

17.1 INTRODUCTION

Natural rubber (NR) is a natural polymeric material collected from *Hevea brasiliensis* or Guayule. Since the first vulcanized natural rubber factory was established in 1839, NR has been used extensively in tires, hoses, belts, shoes, sealing products, vibration insulators, sports and medical products, and adhesives, as well as in military and high-technology fields.

The production of synthetic rubbers in 1930s ended the single contribution of NR in the rubber industry. With the rapid development of the petrochemical industry from the 1950s, the yield of synthesized rubbers exceeded that of natural rubber. Currently, the relative yields of natural rubber and synthesized rubber are approximately 40% and 60%, respectively. However, synthetic rubbers come from nonrenewable petroleum resources, and the production process is energy-intensive and polluting. With the increasing depletion of petroleum resources, the importance and developable potential of NR as a green, renewable, and degradable elastomer material for environment concerns and sustainable development will increase (Anil and Howard, 2001).

Natural rubber has the molecule structure of *cis*-1,4-polyisoprene. Generally, its molecular weight is in range 10^4-10^7, and the index of molecular weight distribution is from 2.5 to 10 (Anil and Howard, 2001). With the high flexibility of NR molecular chains, the material exhibits excellent elasticity, high fatigue resistance, and low hysteresis loss. At the same time, the high stereoregularity of the NR molecular structure affords tensile crystallization and orientation, which leads to a self-reinforcing action and hence lead to high tensile strength, tear strength, abrasive resistance, and so on. In addition, NR has excellent processability.

Ordinarily, the properties of NR pure gum vulcanizate cannot satisfy the requirements of rubber products. Reinforcing agents have to be added to increase the hardness, modulus, tear strength, tensile strength, abrasive resistance, fatigue resistance, etc. The traditional reinforcing agent for NR and other rubbers is carbon black. The dosage of carbon black can reach 50–60% of the amount of rubber. As well as carbon black, silica and certain resins can be used as reinforcing agents. Some inert fillers, such as clay, calcium carbonate, and talcum, are also usually added to rubber compounds. These do not play a role in the reinforcement of the rubber and are applied only to increase the volume and decrease cost (Dick, 2001).

Since the latter part of the twentieth century, along with the development of nanotechnology around the world, research on rubber-based nanocomposites reinforced with nanometer particles such as montmorillonite, kaolin, nano-calcium carbonate, nanosilica, nano-magnesium hydroxide, attapulgite clay, and halloysite, has attracted great interest in rubber science and technology. The common features of these nanocomposites are that they do not depend on petroleum, and that most of the raw materials are of natural occurrence or are prepared from natural resources that are of low cost. The price of NR has soared because of the effects of natural disasters and the like; and the price of carbon black, which is mostly made from petroleum, has also increased significantly. Therefore, research on NR-based

nanocomposites reinforced with cheap natural nano-fillers is important for the manufacture of rubber products that have low cost and high performance as well as being environmentally friendly and offering sustainable development.

Polymer layered silicate (PLS) nanocomposites are hybrids consisting of an organic phase (the polymer) and an inorganic phase (the silicate). The choice of the silicate determines the nanoscopic dispersion of the nanocomposites. The silicates employed belong to the family of layered silicates known as phyllosilicates, such as mica, talc, montmorillonite, vermiculite, hectorite, and saponite. They belong to the general family of so-called 2 : 1 layered silicates. Their crystal structure consists of layers made up of two silica tetrahedra fused to an edge-shared octahedral sheet of either alumina or magnesia. Stacking of the layers leads to a regular van der Waals gap between the layers called the interlayer or gallery. Isomorphic substitution within the layers generates negative charges that are normally counterbalanced by cations residing in the interlayer (Utracki et al., 2007).

Pristine layered silicates usually contain hydrated sodium or potassium ions. Ion-exchange reactions with cationic surfactants render the normally hydrophilic silicate surface organophilic, which makes possible the intercalation of many engineering polymers. The role of alkylammonium cations in the organosilicates is to lower the surface energy of the inorganic component and improve the wetting characteristics with the polymer. Additionally, the alkylammonium cations can provide functional groups that can react with the polymer or initiate polymerization of monomers to improve the strength of the interface between the inorganic component and the polymer (Utracki et al., 2007; Okada and Usuki, 2006; Alexandre and Dubois, 2000; LeBaron et al., 1999; Giannelis, 1998).

In general, two types of hybrid structures are possible: intercalated, in which a single, extended polymer chain is intercalated between the silicate layers, resulting in a well-ordered multilayer with alternating polymer/inorganic layers; and disordered or delaminated, in which the silicate layers (1 nm thick) are exfoliated and dispersed in a continuous polymer matrix. It was not until 1988 that the first industrial application was provided by Okada and co-workers at Toyota's central research laboratories in Japan. In this case a Nylon 6 nanocomposite was formed by polymerization in the presence of the inserted monomer. It is currently used to make the timing belt cover of Toyota's car engines and for the production of packaging film (Kojima et al., 1993b; Okada et al., 1988; Pinnavaia et al., 2001). Since then, much work has been done on polymer/silicate nanocomposites worldwide.

Since the 1980s, with the development of the technology of intercalating nanocomposites polymers and inorganics, clay fillers with nanolayered structure, for example, montmorillonite, allowed dispersion on the nanometer scale in rubber matrix and hence led to the formation of rubber/clay nanocomposites, in which clay has remarkable reinforcing effects on the rubber matrix. The barrier properties, thermal stability, aging resistance, and flammability resistance of rubber were also improved. Okada and co-workers (Okada et al., 1995; Kojima et al., 1993a) reported that only 10 phr of organoclay was required in Nitrile Butadiene Rubber (NBR) to achieve tensile strength comparable to that of the compound containing 40 phr of

carbon black. The permeability of hydrogen and water decreased to 70% with addition of 3.9% w/w montmorillonite. These rubber-based nanocomposites can be used as tire inner-liners.

The preparation of the rubber/clay nanocomposites typically involved the intercalation of rubber in the organoclay during mixing, in the latex or in solution state (Okada et al., 1991; Burnside and Giannelis, 1995; Laus et al., 1997; Wang and Pinnavaia, 1998; Wang et al., 1998; Zhang et al., 2000a,b; Arroyo et al., 2003; Jeon et al., 2003; Gatos et al., 2004; López-Manchado et al., 2004; Zheng et al., 2004). In these conditions, the surfaces of clay layers are sufficiently compatible with the rubber that the rubber molecular chains can infiltrate into the interlayer space of the clay and form either intercalated or exfoliated nanocomposites. However, the layers of clay dispersing in rubber/clay nanocomposites always form aggregates with an average thickness in the range of about 10–200 nm because the poor interfacial adhesion between the rubber and the layers of clay causes ten or more layers to congregate together. It is therefore important to enhance the interfacial adhesion between the inorganic layers and the rubber matrix.

In this chapter, the results of the authors' research on nanocomposites of NR and a typical clay filler, montmorillonite, are reviewed.

17.2 MATERIALS AND PROCESS

17.2.1 Materials

Natural rubber latex with 60 wt% of solid content was produced in Hainan province, China; Natural Rubber with trade name ISNR-3 was supplied from Thailand. Na-montmorillonite (MMT), with a cationic exchange capacity of 90 meq/100 g, was supplied by Nanhai Inorganic Materials Factory, China. Modified organomontmorillonites USMMT, HMMT, GMMT, AMMT were prepared by a solid-phase method in our laboratory (Jia et al., 2002; Wang and Jia, 2004) (See later for the specification of these compounds); resorcinol and hexamethylenetetramine complex (RH) was supplied by Zhujiang Tire Corp., China. Butyl acrylate (BA) monomer and other reagents were of pure chemicals grade.

17.2.2 Processing and Procedures

Preparation of NR/BA/USMMT Nanocomposites by Grafting and Intercalating Method in Latex NR latex, USMMT aqueous suspension, BA monomer, the initiator potassium persulfate, and the surfactant sodium dodecyl sulfate were mixed and stirred for 2 h at room temperature, and then the mixture was reacted for 6 h at 80°C. Electrolyte was added to co-coagulate the mixture. The coagulum was washed several times with water and dried in an oven at 60°C, and finally the NR/BA/USMMT compound was obtained.

The coagulated NR/BA/USMMT compound and other ingredients were mixed on a 160 mm-diameter open roll mill by a common procedure and then the compound

was cured in a compression mold at 143°C. The optimum cure time was determined by RPA 2000 Rubber Process Analyzer (Alpha Technologies, USA).

Preparation of NR/HMMT/RH Nanocomposite by Grafting and Intercalating Method in Mixing and Curing Process NR, organomodified montmorillonite HMMT, RH complex, and other rubber ingredients were mixed on a 160 mm-diameter two-roll mill by a common procedure. The compound was vulcanized in an electrically heated press at 143°C. The optimum cure time t_{90} was determined by RPA 2000 Rubber Process Analyzer.

Preparation of NR/GMMT Nanocomposite by Reacting and Intercalating Method in Mixing and Curing Process NR and organomodified montmorillonite GMMT with multiple sulfur bonds as well as other ingredients were mixed on a 160 mm-diameter two-roll mill by a common procedure and the compound was vulcanized in an electrically heated press at 143°C for the optimum cure time t_{90}.

17.3 CHARACTERIZATION

17.3.1 X-Ray Diffraction

X-ray diffraction analysis was performed with the D/MAX-III power diffractometer using CuKα radiation ($\lambda = 1.54$ Å) and a curved crystal graphite monochromator.

17.3.2 Dynamic Mechanical Analysis

A TA Instruments Universal V1.7F DMA2980 instrument was used for dynamic mechanical analysis (DMA) in the tension mode on a sample of approximately 6 mm width and 1.5 mm height. Temperature scans from −120°C to 200°C were carried out at a heating rate of 3°C/min and frequency of 10 Hz.

17.3.3 Transmission Electron Microscopy

Transmission electron microscopy observation was performed with a JEOL JEM-100SX microscope using an acceleration voltage of 80 kV. The samples were prepared using an ultramicrotome in a liquid-nitrogen trap.

17.3.4 Mechanical Properties and Aging Resistance Testing

Mechanical properties testing and aging resistance testing were performed according to the relevant Chinese Standards (GB). Tensile tests were measured using a Shimadzu AG-I tensile machine with an extension rate of 500 mm/min at room temperature.

17.3.5 Rubber Process Analyzer

A Rubber Process Analyzer RPA 2000 (Alpha Technologies) was used to determine the curing characteristics of unvulcanized rubber and measure the mechanical loss factor of vulcanized rubber at frequencies from 0.5 to 25 Hz with 0.5 degree strain at 50–100°C.

17.4 RESULTS AND DISCUSSION

17.4.1 Solid-Phase Method for Modification of Montmorillonite

The organic modification of montmorillonite is usually achieved in aqueous suspension system, and requires complex processes such as decentralization, swelling, heat, reaction, filtering, washing, drying, grinding, and so on. The complexity of this method leads to high prices and pollutes the environment and also hinders the application of polymer/montmorillonite nanocomposites. Accordingly, the authors have successfully developed a new technique, intercalation of montmorillonite in the solid state, in which the montmorillonite in the solid state is mixed with organic modifiers, stirred, and heated. This greatly simplifies the process of montmorillonite intercalation, significantly reduces the cost, and is nonpolluting, which is conducive to industrialization and wider utilization.

Six kinds of solid-phase intercalated montmorillonites have been developed: (1) USMMT, which was intercalated with unsaturated chemicals with C═C double bonds; (2) UAMMT, which was intercalated with long-chain nonpolar organics; (3) EMMT, which was intercalated with chemicals with epoxy groups; (4) AMMT, which was intercalated with chemicals with amido groups; (5) TMMT, which was intercalated with chemicals with phosphate groups; (6) GMMT, which was intercalated with chemicals with multiple sulfur bonds (Liu et al., 2002a,b, 2004, 2006a,b; Wang et al., 2004).

17.4.2 Natural Rubber/Montmorillonite Nanocomposites Prepared by Grafting and Intercalating Method in Latex

Rubber/clay nanocomposites have attracted considerable research attention due to their outstanding mechanical properties, thermal stability, and barrier properties. The

TABLE 17-1 d_{001} Values of Solid-Phase-Modified Montmorillonite Determined by XRD (Liu et al., 2004, 2006a,b; Wang et al., 2004)

	2θ (°)	d_{001} (nm)
MMT	6.90	1.25
USMMT	4.90	1.76
UAMMT	2.48	3.80
AMMT	6.90	1.25
	3.31	2.62
EMMT	6.90	1.25
	2.55	3.37
TMMT	5.76	1.53
GMMT	1.52	5.81

preparation of the rubber/clay nanocomposites typically involved the intercalation of rubber in the organoclay in mixing, in the latex or in solution state, which requires that the surfaces of clay layers are sufficiently compatible with the rubber that the rubber molecular chains can infiltrate into the interlayer space of the clay and form either intercalated or exfoliated nanocomposites. Several studies have been undertaken to prepare rubber/clay nanocomposites in latex by co-coagulating rubber latex and clay aqueous suspension (Wu et al., 2001; Jia et al., 2002; Liu et al., 2002).

In this work, NR/montmorillonite nanocomposites were prepared in latex by a grafting and intercalating method (Liu et al., 2006), in which an organomontmorillonite with unsaturated carbon–carbon double bonds on the interlayer surfaces (USMMT) and a monomer, butyl acrylate (BA), were added to NR latex and reacted for some time under appropriate conditions; then the latex mixture was co-coagulated and dried. The grafting and intercalating method in latex is shown schematically in Fig. 17-1. It is expected that the monomers can intercalate into the interlayer galleries of USMMT and polymerize in situ together with C=C bonds on the interlayer surfaces and, at the same time, the monomers can undergo grafting copolymerization onto NR molecular chains and form a conjugated three-component interpenetrating network structure (Jia et al., 1991, 1994). Consequently the interfacial combination between the layered silicate and rubber should be strengthened and the mechanical properties of the nanocomposites should be improved. This is a novel way of preparing rubber/organoclay nanocomposites.

XRD was used to measure the change of the interlayer spacing of the silicate before and after introducing the monomer BA, and the results are shown in Fig. 17-2. The results show that the XRD patterns of USMMT contain a peak at $2\theta = 4.9^\circ$, while a strong peak at $2\theta = 2.18^\circ$ is observed in the NR/BA/USMMT (100/10/5) nanocomposite, which is a basal reflection from the silicate layers. The d_{001} values of USMMT and NR/BA/USMMT (100/10/5) are 1.8 nm and 4.0 nm, respectively, indicating that some polymer chains intercalate into the galleries of USMMT; the monomer BA was added to participate in the polymerization in situ in the rubber matrix. The d_{001} value of NR/BA/USMMT (100/10/10) reaches 4.2 nm, which means that more macromolecular chains could intercalate into the

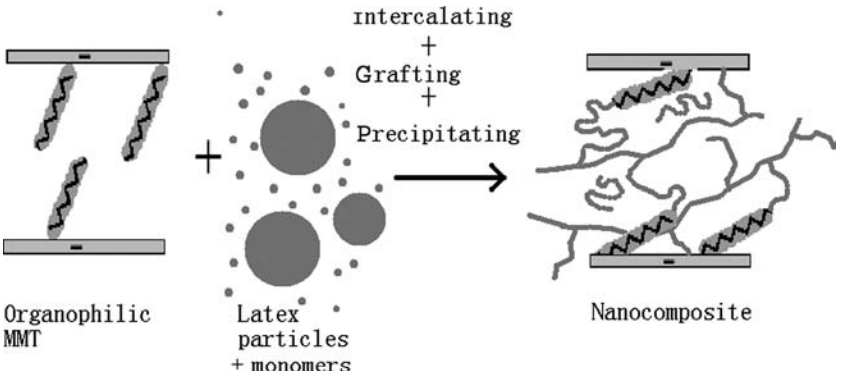

Fig. 17-1 Schematic of the method of grafting and intercalating in latex.

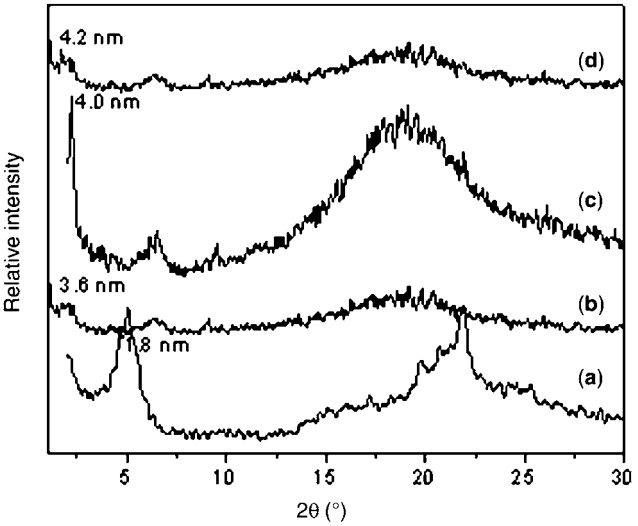

Fig. 17-2 XRD curves of NR/MMT nanocomposites by grafting and intercalating method in latex. (a) USMMT (d_{001}=1.8 nm); (b) NR/USMMT(100/10) (d_{001}= 3.6nm); (c) NR/BA/USMMT (100/10/5) (d_{001}= 4.0nm); (d) NR/BA/USMMT(100/10/10) (d_{001}= 4.2nm).

galleries. The XRD results show that monomer BA can intercalate into the interlayer galleries of modified clay and polymerize in situ, and at the same time graft onto NR through emulsion polymerization.

The mechanical properties of the nanocomposites are summarized in Table 17-2. Compared with the NR, NR/BA and NR/USMMT nanocomposites, the mechanical properties of NR/BA/USMMT nanocomposites are clearly improved in 300% and 500% modulus, tensile strength, and tear strength while good elasticity is still retained. As discussed above, the chains of NR can intercalate into modified clay galleries in the latex state and monomer BA can connect the rubber chains and layers of

TABLE 17-2 Mechanical Properties of the Vulcanizates of NR, NR/USMMT, and NR/BA/USMMT Composites

	NR	NR/BA	NR/ USMMT	NR/BA/ USMMT	NR/BA/ USMMT
NR	100	100	100	100	100
USMMT	–	–	5	5	5
BA	–	10		5	10
300% modulus (MPa)	2.78	2.72	2.90	3.89	3.94
500% modulus (MPa)	4.85	5.63	5.04	7.54	7.62
Tensile strength (MPa)	17.56	22.38	21.43	24.38	26.41
Elongation at break (%)	800	800	750	900	800
Tear strength (kN/m)	24.62	27.14	25.71	30.45	29.61
Hardness (Shore A)	37	40	44	40	44

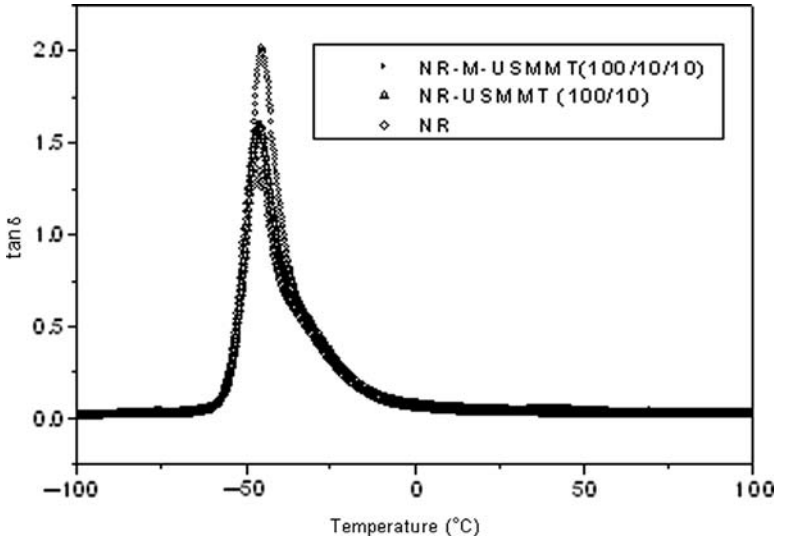

Fig. 17-3 DMA spectra of NR, NR/USMMT, and NR/BA/USMMT nanocomposites.

clay through polymerization in situ. As a result, the interfacial combination between rubber and clay layers is enhanced and the mechanical properties of NR are improved significantly.

Dynamic losses are usually associated with hysteresis and some mechanism of molecular or structural motion in rubber materials. The damping characteristics are extensively measured as the tangent of the phase angle (tan δ). Figure 17-3 shows the tan δ curves of NR, NR/USMMT, and NR/BA/USMMT nanocomposites and the T_g and tan δ values at 0°C and 60°C of NR/BA/USMMT system are shown in Table 17-3. NR exhibits T_g at −46.9°C. The T_g of NR/BA/USMMT nanocomposite increases to −45.3°C due to the interaction between the layers and the chains of rubber through the grafting and intercalation of BA. It is known that for tire applications, high tan δ of the vulcanizate at 0°C is favorable for wet grip, and a low tan δ at 60°C is favorable for reducing rolling resistance. From Table 17-3, the tan δ value of NR/BA/USMMT nanocomposites at 60°C is lower than that of NR, which means the NR/BA/USMMT nanocomposite has a lower rolling loss.

TABLE 17-3 The T_g Values of the NR/USM/BA System from DMA

	T_g (°C)	tan δ (0°C)	tan δ (60°C)
NR	−46.9	0.073	0.036
NR/USM (100/10)	−46.1	0.078	0.034
NBR/USM/BA (100/10/10)	−45.3	0.048	0.013

17.4.3 Natural Rubber/Montmorillonite Nanocomposites Prepared by Grafting and Intercalating Method in Mixing and Curing Process

The solution intercalation method needs a compatible rubber-solvent system and modified organoclay. Its disadvantages are the environment pollution due to the solvents and the difficulty of removing the solvents. In latex intercalation it is necessary to co-coagulate the rubber latex and clay suspension and then dry the mixture. The procedure is complicated. Compared with the latex and solution intercalation method, the method of mechanical mixing intercalation is a convenient and easy way to realize industrialization. The approach is suitable to produce rubber-based nanocomposites and it can be applied to most rubbers.

In general, however, only some segments of the rubber macromolecules can intercalate into the interlayer galleries of the clay in the mixing intercalation method since rubber is a high-molecular-weight polymer with very high viscosity in the processing state and has very poor interfacial adhesion with the layers of clay.

In our previous work (Liu et al., 2002a,b; Jia et al., 2002), a new method for preparing rubber/clay nanocomposites by introducing some monomers into the NR latex/organoclay system was investigated. This method can enhance the interfacial adhesion between the inorganic layers and the rubber matrix so that the mechanical properties of NR/organoclay nanocomposites are greatly improved. However, this latex intercalation needs to polymerize the monomer and then co-coagulate the rubber latex and organoclay. The procedure is still complicated.

In this section, the authors develop a new preparation method for rubber/clay nanocomposites, which we term the grafting and intercalating method in mixing and curing process, by introducing some reactive monomers during the rubber mixing and vulcanization process. The organomontmorillonite (HMMT) was prepared by ion exchanging Na^+-MMT with hexadecyltrimethylammonium bromide. The monomer adopted was resorcinol and hexamethylenetetramine complex (RH; the structural formula is shown in Scheme 17-1). RH is an usual adhesive in the rubber industry; it can be decomposed into resorcinol and formaldehyde at temperatures above 110°C and can react with NR in the process of vulcanization (Jain and Nando, 1988). It was expected that RH would intercalate into the interlayer galleries of HMMT and polymerize in situ while RH and NR are reacting; consequently the interfacial combination between rubber and the layered silicate should be strengthened

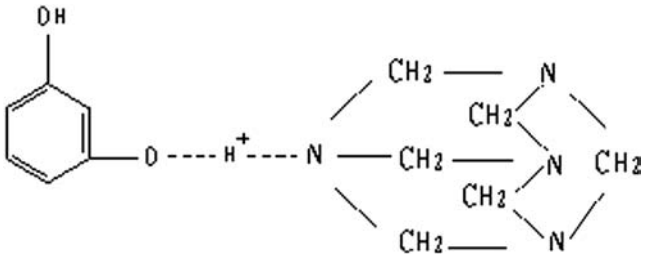

Scheme 17-1 Structural formula of RH.

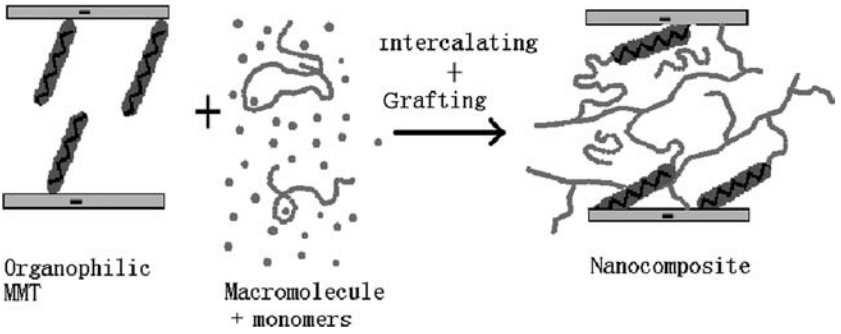

Fig. 17-4 Schematic of the reactive mixing intercalation method.

and the mechanical properties of the nanocomposites should be improved. The reactive mixing intercalation method is shown schematically in Fig. 17-4.

Table 17-4 lists the mechanical properties of the NR vulcanizate and its composites. Compared with neat NR, the mechanical properties of NR/HMMT nanocomposites increase dramatically. With the addition of RH, the mechanical properties of NR/HMMT/RH nanocomposites are further improved for 300% modulus, tensile strength, tear strength, and elongation at break. Furthermore, the results of aging tests demonstrate that the mechanical properties of NR/HMMT/RH nanocomposites after aging in air for 48 h at $100 \pm 1^{\circ}C$ are better than those of NR/HMMT nanocomposites. The results show that the reaction and interactions of RH with NR and HMMT can improve the interfacial adhesion between NR and silicate layers and facilitate dispersion of the silicate layers in the rubber matrix at nanometer level. The high aspect ratio characteristic of silicate layers in nanocomposites can not only reinforce the rubber but also strongly reduce the hot air permeability, which can protect the macromolecules from thermal and oxidative aging.

The tan δ values at 0°C and 60°C are also summarized in Table 17-4. The tan δ value of NR/HMMT/RH nanocomposites is higher at 0°C and lower at 60°C,

TABLE 17-4 Mechanical Properties of NR/NR/HMMT and NR/HMMT/RH Vulcanizates (Liu et al., 2004, 2006a,b)

	NR	NR/HMMT (100/10)	NR/HMMT/RH (100/10/8)
d_{001} of MMT/nm	–	2.6	5.5
Modulus at 300% (MPa)	1.36	1.62	2.11
Tensile strength (MPa)	17.60	19.44	26.34
Elongation at break (%)	800	750	900
Tear strength (kN/m)	28.72	26.74	35.72
Hardness (Shore A)	35	38	44
tan δ at 60°C	0.036	0.037	0.026
tan δ at 0°C	0.075	0.110	0.089
Property descend ratio after aging in air (%) ($100 \pm 1^{\circ}C$; 48 h)	46.0	40.7	30.9

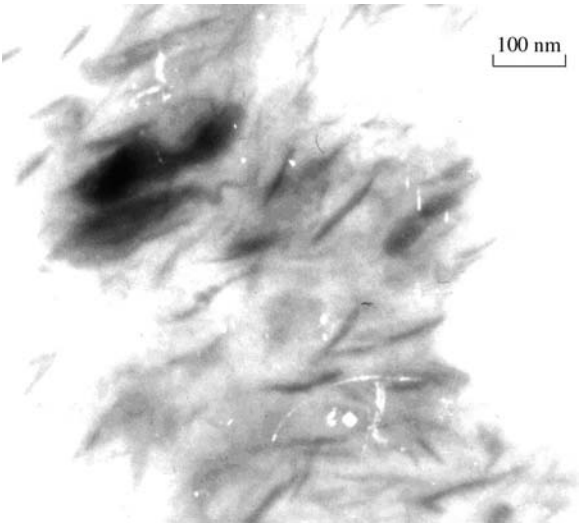

Fig. 17-5 TEM image of NR/RH/HMMT nanocomposite.

indicating that the nanocomposites have better damping properties around room temperature and lower heat build-up at higher temperature.

Figure 17-5 shows a TEM image of NR/HMMT/RH nanocomposite. The dark lines in the micrographs correspond to the intersections of the silicate layer. It is apparent that the layered silicate is further divided into thinner bundles with thicknesses of 5–20 nm and lengths of about 100 nm dispersed uniformly in rubber matrix, and there are still individual larger aggregates with sizes of more than 50 nm. The preparation of NR/HMMT/RH nanocomposites may be considered successful due to the addition of RH. RH improved the dispersion of HMMT in the rubber matrix and the interfacial adhesion between rubber macromolecule chains and silicate layers, and hence increased the intercalation efficiency.

17.4.4 Natural Rubber/Montmorillonite Nanocomposites Prepared by Reacting and Intercalating Method in Mixing and Curing Process

Compared with ordinary mixing intercalation, the intercalating effect of the mechanical mixing and grafting intercalation method is a clear improvement; however, the adding of suitable monomers is inconvenient for processing. Accordingly, a new technique termed the mechanical mixing and reaction intercalation method was developed by us (Wang et al., 2004). In this technique, first, in the course of the organic modification of montmorillonite by the solid-state method, some reactive groups are introduced onto the interlayer surfaces of montmorillonite; and then in the course of mechanical mixing and vulcanization of the rubber compound, NR macromolecules intercalate into the interlayers of montmorillonite by mechanical

TABLE 17-5 The Effect of Organomontmorillonite Amount on the Mechanical Properties of NR/GMMT Composities (Wang, 2004)

NR (pph)	100	100	100	100	100	100
GMMT (pph)	0	2	4	6	8	10
100% modulus (MPa)	0.82	0.77	0.89	1.01	1.17	1.44
300% modulus (MPa)	1.83	2.21	2.39	3.15	3.61	5.53
Tensile strength (MPa)	20.3	25.3	27.1	28.9	26.3	26.0
Elongation at break (%)	610	708	698	682	678	610
Permament set (%)	12	18	22	25	30	32
Tear strength (kN/m)	22.4	25.2	30.1	30.5	31.7	30.9
Shore A hardness (degrees)	35	37	38	40	42	45
Descend ratio of mechanical properties after aging (100°C; 48 h)	44.32	40.99	37.64	25.76	30.65	32.64

shear, compression, and thermochemical effects and react in situ with the reactive groups. The reactive intercalation leads to fine dispersion of montmorillonite in the rubber matrix at nanometer scale and enhances the interfacial combination between rubber and montmorillonite; hence, NR/montmorillonite nanocomposites with high performance are obtained. This new technique has good applicability prospects in industry with advantages of simple technology, low cost, and high efficiency of intercalation.

The mechanical properties and aging resistance of NR/GMMT nanocomposites prepared by the mechanical mixing and reaction intercalation method are listed in Table 17-5. The results show that the modulus, tensile strength, elongation at break, and tear strength of the nanocomposites are evidently improved; at the same time, the aging resistance is distinctly enhanced.

The TEM image of an NR/GMMT nanocomposite in Fig. 17-6 shows the modified montmorillonite dispersed in the rubber matrix at several to tens of nanometers,

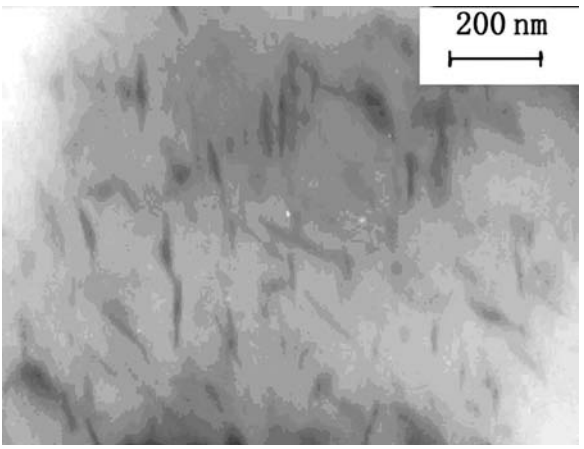

Fig. 17-6 TEM image of NR/GMMT (100/10) nanocomposite.

mostly less than 10 nm. A typical sandwich structure consisting of parallel alternating organoclay layers and rubber matrix indicates the coexistence of intercalated/exfoliated clay structure.

Figure 17-7 summarizes the change in properties of NR/AMMT nanocomposite after aging in air at 100°C. It is clear that the addition of modified montmorillonite significantly improves the mechanical properties in aging. NR/AMMT nanocomposite maintains about 67% of tensile strength and 68% of elongation at break after aging for 7 days. However, for the blank sample without montmorillonite the values are 26% and 27%, respectively.

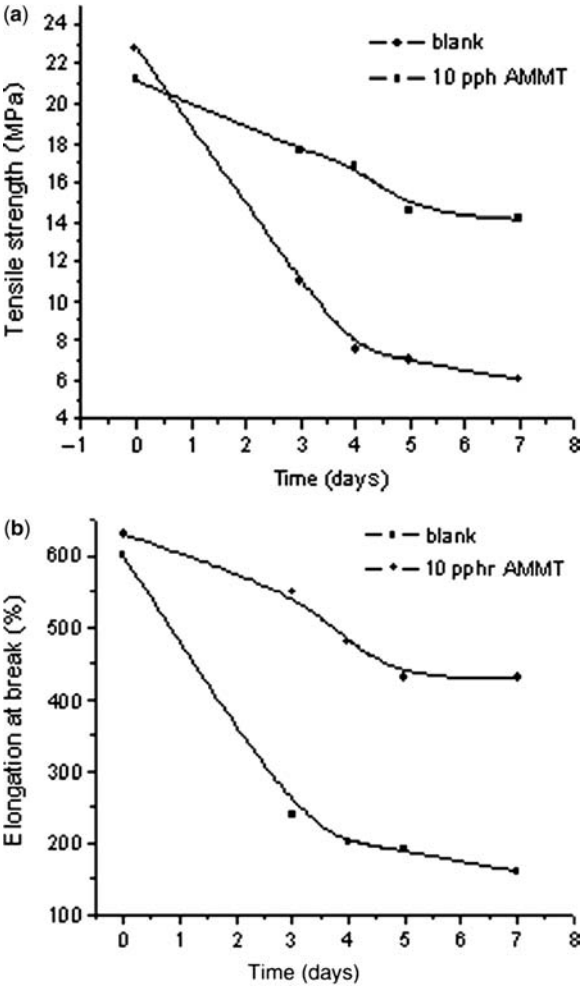

Fig. 17-7 The aging behavior of NR/AMMT (100/10) nanocomposites (100°C, in air). (a) Tensile strength and (b) elongation at break against aging time.

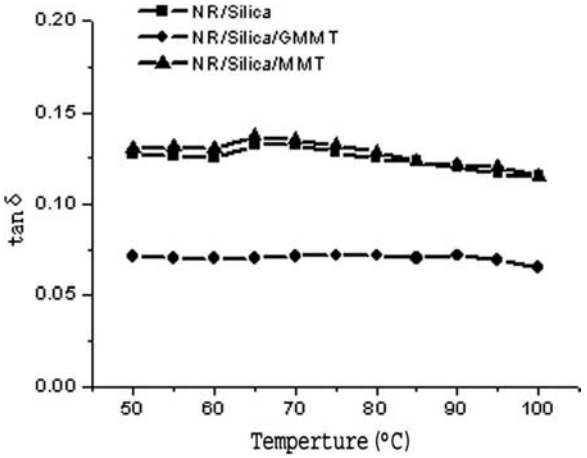

Fig. 17-8 The temperature sweep curves of NR/silica/GMMT nanocomposite and related materials.

The RPA temperature sweep curves of NR/silica/GMMT, NR/silica/MMT, and NR/silica composites shown in Fig. 17-8 show that the damping coefficient of NR/silica/GMMT nanocomposites in range 50–100°C is lower than that of NR/silica and NR/silica/MMT composites. This indicates that the heat-build and rolling resistance of NR/silica/GMMT nanocomposites is the lowest of the three materials. This behavior is quite valuable for rubber products working in dynamic conditions, such as tire and vibration-damping products.

Much work has been done to study the flammability properties of different kinds of polymer/clay nanocomposites using the cone calorimeter, and it is found that clay fillers could become a popular "green" alternative to current flame-retardant additives for polymers. Cone calorimeter data showed that both the peak and average heat release rate (HRR), were reduced significantly for intercalated and delaminated nanocomposites with low silicate mass fraction of 2–5% where no additional flame retardant is used (Gilman et al., 1998). The flammability properties of rubber/layered silicate nanocomposites systems have been much less reported in the literature (Song et al., 2005).

NR/organic-modified layered silicate TMMT nanocomposites prepared by the mixing intercalation method and the structure and flame-retardant properties of the nanocomposites were studied. The samples were analyzed by cone calorimeter to compare the effects of TMMT on polymer flammability, and the results are summarized in Table 17-6. Compared with the NR control, all the samples show reduced HRR and peak HRR values. However, the NR-TMMT nanocomposites show larger reduction in HRR than do NR-MMT microcomposites. The results in Table 17-6 show that when the mass fraction of TMMT is 10 pph, the peak HRR of NR-TMMT nanocomposites is reduced by 44%; the peak HRRs are further reduced as the mass fraction of TMMT increases. When the mass of TMMT is

TABLE 17-6 Cone Calorimeter Results for NR, NR/MMT Composites and NR/TMMT Nanocomposites

	NR	NR-MMT Microcomposites	NR-TMMT Nanocomposites		
MMT	–	10	–	–	–
TMMT	–	–	10	20	30
Tig (s)	29	26	25	32	27
Peak HRR (kW/m^2)	1222	732	679	577	644
Average HRR (kW/m^2)	630	508	472	382	365

increased to 20 wt%, the peak HRR of the NR-TMMT nanocomposites is 53% lower than that of pure NR (Liu et al., 2008).

The flame retardancy mechanism can be deduced from the cone calorimeter data of NR-TMMT nanocomposites, combined with previous literature reports (Zanetti et al., 2002; Song et al., 2005). Once the nanocomposite is ignited, it burns slowly but does not self-extinguish until most of the fuel has been combusted. The nanodispersed layers of clay collapse down to form a clay-rich barrier that slows the pyrolysis of decomposing polymer and reduces the smoke produced, and at the same time, the tributyl phosphate situated in interlayers of TMMT reacts with decomposition products of NR and layers of clay to form a glassy coat and stable carbonaceous-silicious-phosphorated charred layers. This stable physical protective barrier on the surface of the polymer materials may insulate the underlying polymeric substrate from the heat source and retard heat and mass transfer between the gaseous and condensed phases.

17.5 SUMMARY

Natural rubber is an important renewable and degradable natural elastomer material. Montmorillonite is a cheap natural nanometer material. NR/montmorillonite nanocomposites as complete natural nanocomposites are important for the application of nanometer materials and for environmentally friendly and sustainable development.

Organic modification of montmorillonite in the solid phase is an effective new technique. It can greatly simplify the process of organic modification of montmorillonite, significantly reduce the cost, and reduce pollution, all of which favor the promotion of industrialization and utilization.

In the NR/montmorillonite nanocomposites prepared by grafting and intercalating method in latex, the monomer intercalated into the interlayer galleries of montmorillonite and polymerized in situ on the interlayer surfaces and, at the same time, the monomer underwent grafting copolymerization onto NR molecular chains; consequently the interfacial combination between the layered silicate and NR was strengthened and the mechanical properties of the nanocomposites were remarkably improved.

The grafting and intercalating method in mixing and curing process for preparation of rubber/montmorillonite nanocomposites is a convenient and easy way to realize industrialization. The reactive monomer intercalated into the interlayer galleries of montmorillonite and polymerized in situ while the monomer and NR was reacting and grafting; consequently the interfacial combination between rubber and the layered silicate was again strengthened and the mechanical properties of the nanocomposites were improved. The mechanical mixing and grafting intercalation method is applicable to the production of rubber-based nanocomposites.

The reacting and intercalating method in mixing and curing process for preparing NR/MMT nanocomposites is a novel technique. In this process, NR macromolecules intercalate into the interlayers of montmorillonite and react in situ with the reactive groups in the interlayers, leading to fine dispersion of montmorillonite in the rubber matrix at nanometer scale and enhancing the interfacial combination between rubber and montmorillonite; hence NR/montmorillonite nanocomposites with high performance are obtained. This new technique has good application prospects in industry for its advantages of simple technology, low cost, and high efficiency of intercalation.

Thus, due to enhanced the interfacial adhesion between the inorganic layers and the rubber matrix, the rubber/clay nanocomposites show improved mechanical properties, thermal properties, and gas barrier performance, and reduced flammability when compared with conventional filled polymers.

ACKNOWLEDGMENTS

This work was supported by the National Natural Science Foundation of China (Grants No. 59933060 and No. 50573021).

REFERENCES

Alexandre M, Dubois P. 2000. Polymer-layered silicate nanocomposites: preparation, properties and uses of a new class of materials. *Mater Sci Eng* 28:1.

Anil KB, Howard LS. 2001. *Handbook of Elastomers*. New York: Marcel Dekker.

Arroyo M, López-Manchado MA, Herrero B. 2003. Organo-montmorillonite as substitute of carbon black in natural rubber compounds. *Polymer* 44(8):2447.

Burnside SD, Giannelis EP. 1995. Synthesis and properties of new poly(dimethylsiloxane) nanocomposites. *Chem Mater* 7:1597.

Dick JS. 2001. *Rubber Technology: Compounding and Testing for Performance*. Munich: Hanser.

Gatos KG, Thomann R, Karger-Kocsis J. 2004. Characteristics of ethylene propylene diene monomer rubber/organoclay nanocomposites resulting from different processing conditions and formulations. *Polym Int* 53(8):1191.

Giannelis EP. 1996. Polymer layered silicate nanocomposites. *Adv Mater* 8(1):29–35.

Giannelis EP. 1998. *Appl Organometal Chem* 12:675–680.

Gilman JW, Kashiwagi T, Lomakin S, et al. 1998. *Fire Retardancy of Polymers: the Use of Intumescence*. Cambridge: The Royal Society of Chemistry.

Jain R, Nando GB. 1988. A novel system for nylon-6 tire cord-to-natural rubber adhesion. *Rubber World* 199(2):40–43.

Jeon HS, Rameshwaram JK. 2003. Characterization of polyisoprene-clay nanocomposites prepared by solution blending. *Polymer* 44(19):5749.

Jia DM, Pang YX, Dai ZS. 1991. Conjugate three-component interpenetrating polymer networks and their applications. *Polym Mater Sci Eng* 65:167.

Jia DM, Pang YX, Liang X. 1994. Mechanism of adhesion of polyurethane/polymethacrylate simultaneous interpenetrating networks adhesives to polymer substrates. *J Polym Sci: Part B Polym Phys* 32:817.

Jia DM, Luo YF, Liu L, Zheng ZY. 2002. Rubber-layered silicate nanocomposites and their preparation method. China Patent ZL02134581.3.

Kojima Y, Fukumori K, Okada A, Kurachi T. 1993a. Gas permeabilities in rubber-clay hybrid. *J Mater Sci Lett* 12(12):889–890.

Kojima Y, Usuki A, Kawasumi M, et al. 1993b. Mechanical properties of nylon-6-clay hybrid. *J Mater Res* 6:1185.

Laus M, Francesangeli O, Sandrolini F. 1997. New hybrid nanocomposites based on an organophilic clay and poly(styrene-*b*-butadiene) copolymers. *J Mater Res* 12:3134.

LeBaron PC, Wany Z, Pinnavaia TJ, 1999. Polymer-layered silicate nanocomposites: an overview. *Applied Clay Science* 15:11–29.

Lei Song, Yuan Hu, Yong Tang, Rui Zhang, Zuyao Chen, Weicheng Fan. 2005. Study on the properties of flame retardant polyurethane/organoclay nanocomposites. *Polym Degrad Stab* 87:111–116.

Liu L, Luo YF, Jia DM. 2008. Flammability properties of NR-organoclay nanocomposites. *Polymer Composites* (in press).

Liu L, Luo YF, Zhang F, Huang MY, Jia DM. 2002. Properties of NR/HMMT nanocomposites prepared by intercalation in latex. *China Synthetic Rubber Industry* 25(4):262.

Liu L, Luo YF, Jia DM, Fu WW, Guo BC. 2004. Studies on NBR-ZDMA-OMMT nanocomposites prepared by reactive mixing intercalation method. *Int Polym Process* 12:374.

Liu L, Luo YF, Jia DM, Fu WW, Guo BC. 2006a. Preparation, structure and properties of nitrile-butadiene rubber-organoclay nanocomposites by reactive mixing intercalation method. *J Appl Polym Sci* 100(3):1905.

Liu L, Luo YF, Jia DM, Fu WW, Guo BC. 2006b. Structure and properties of natural rubber-organoclay nanocomposites prepared by grafting and intercalating method in latex. *J Elastomers Plast* 38(2):147–161.

López-Manchado MA, Herrero B, Arroyo M. 2004. Organoclay-natural rubber nanocomposites synthesized by mechanical and solution mixing methods. *Polym Int*. 53(11):1766.

Okada A, Usuki A. 2006. Twenty years of polymer-clay nanocomposites. *Macromol Mater Eng* 291(12):1449–1476.

Okada A, Fukumori K, Usuki A, Kojima Y, Kurauchi T, Kamigaito O. 1991. Rubber-clay hybrid: synthesis and properties. *Polym Prep* 32:540.

Okada A, Usuki A, Kurauchi T, et al. 1995. *Hybrid Organic-Inorganic Composites*. ACS Symposium Series. p. 55–65.

Okada A, Fukoshima Y, Inagaki S, et al. 1988. US Patent 4,739,007.

Pinnavaia TJ, Beall GW. 2001. *Polymer-Clay Nanocomposites*. Chichester: Wiley.

Utracki LA, Sepehr M, Boccaleri E. 2007. Review of synthetic layered nanoparticles for polymeric nanocomposites. *Polym Adv Technol* 18:1–37.

Wang SJ, Long CF Long, et al. 1998. Synthesis and properties of silicone rubber/organomontmorillonite hybrid nanocomposites. *J Appl Polym Sci* 69(8):1557–1561.

Wang XP, Jia DM. 2004. China Patent 200410051956.0.

Wang, Pinnavaia TJ. 1998. Nanolayer reinforcement of elastomeric polyurethane, *Chem Mater* 10(12):3769–3771.

Wu YP, Zhang LQ, et al. 2001. Structure of CNBR-clay nanocomposites by co-coagulating rubber latex and clay aqueous suspension. *J Appl Polym Sci* 82(11):2842–2848.

Wang YZ, Zhang LQ, et al. 2000. Preparation and characterization of rubber-clay nanocomposites. *J Appl Polym Sci* 78(11):1879–1883.

Zanetti M, Kashiwagi T, Falqui L, Camino G. 2002. Cone calorimeter combustion and gasification studies of polymer layered silicate nanocomposites. *Chem Mater* 14:881–887.

Zheng H, Zhang Y, Peng Z, Zhang Y. 2004. Influence of clay modification on the structure and mechanical properties of EPDM/montmorillonite nanocomposites. *Polym Test* 23(2):217.

Zhang LQ, Wang YZ, et al. 2000a. Morphology and mechanical properties of Clay/SBR nanocomposites. *J Appl Polym Sci* 78(11):1873–1878.

Zhang L, Wang Y, et al. 2000b. Morphology and mechanical properties of clay/styrene-butadiene rubber nanocomposites. *J Appl Polym Sci* 78(11):1873.